Journal Pre-proof

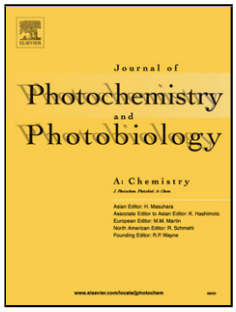

Synthesis, photochemistry and photophysics of new butadiene derivatives: influence of the fluoro, dimethylamino and nitro substituents on the molecular structure and photoinduced behavior

Ana Grgičević, Lajos Fodor, Danijela Barić, Margareta Poje, Željko Marinić, Ottó Horváth, Irena Škorić

PII: S1010-6030(20)30489-5

DOI: https://doi.org/10.1016/j.jphotochem.2020.112690

Reference: JPC 112690

To appear in: *Journal of Photochemistry & Photobiology, A: Chemistry*

Please cite this article as: Grgičević A, Fodor L, Barić D, Poje M, Marinić Ž, Horváth O, Škorić I, Synthesis, photochemistry and photophysics of new butadiene derivatives: influence of the fluoro, dimethylamino and nitro substituents on the molecular structure and photoinduced behavior, *Journal of Photochemistry and amp; Photobiology, A: Chemistry* (2020), doi: https://doi.org/10.1016/j.jphotochem.2020.112690

Synthesis, photochemistry and photophysics of new butadiene derivatives: influence of the fluoro, dimethylamino and nitro substituents on the molecular structure and photoinduced behavior

Ana Grgičević,[a§] Lajos Fodor,[b§] Danijela Barić,[c] Margareta Poje,[a] Željko Marinić,[d] Ottó Horváth,[b,*] horvath.otto@mk.uni-pannon.hu Irena Škorić[a,**] iskoric@fkit.hr

[a]Department of Organic Chemistry, Faculty of Chemical Engineering and Technology, University of Zagreb, 10000 Zagreb, Croatia

[b]Department of General and Inorganic Chemistry, Institute of Chemistry, Faculty of Engineering, University of Pannonia, P.O.B. 158, Veszprém H-8201, Hungary

[c]Division of Physical Chemistry, Rudjer Bošković Institute, Bijenička cesta 54, 10 000 Zagreb, Croatia

[d]NMR Center, Rudjer Bošković Institute, Bijenička cesta 54, 10 000 Zagreb, Croatia

,

[§]These authors contributed equally.

Graphical abstract

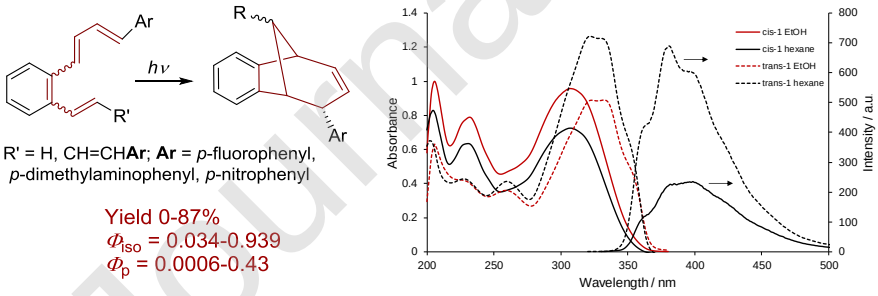

Highlights

- new hexatriene systems with arylbutadiene unit(s), substituted with F, $N(CH_3)_2$ or NO_2 group(s) were synthesized
- diverse photochemistry and photophysics of derivatives were established and explained
- the primary photochemical step for each compound is a fast cis-trans isomerization
- in some cases intramolecular cycloaddition gave photoproducts with bicyclo[3.2.1]-skeleton
- computational investigation of energy profiles of Wittig reaction gave rationalization of stereochemistry

Abstract

Novel *p*-fluoro, *p*-dimethylamino and *p*-nitro substituted arylbutadiene derivatives were synthesized by Wittig reaction and their diverse photochemistry and photophysics were established and explained. Under excitation mono- and difluoro derivatives undergo photoinduced intramolecular cycloaddition. The parent mono-dimethylamino substituted derivative undergoes the same reaction type giving the photocycloadduct in lower yield and with incomplete consumption, whereas its bis(dimethylamino) analogue shows only geometrical isomerization due to the steric effect of the substituents. Mono- and dinitro derivatives show photochemical unreactivity. Conjugated analogues with similar structures display dramatically different photoinduced behavior, revealing how changes of the nature of substituents impact their photophysics and photochemistry. The computational investigation of the effects of the conformational diversity within the steric influence of the starting geometric isomers on the photoreaction pathway and energy profiles of the Wittig reaction is performed for the first time.

Key words: arylbutadiene, photochemistry, photophysics, substituent impact, Wittig reaction

Introduction

The synthesis and photochemistry of 1-(*o*-vinylphenyl)-4-phenylbutadiene derivative **A** and its *ω,ω*'-diarylbutadiene analogue **B** (Figure 1, Ar = Ph), molecules that combine properties of both butadiene and hexatriene systems, were examined and described for the first time by our group.[1] That was the first approach to 4-substituted benzobicyclo-[3.2.1]octadienes as photoproducts from arylbutadiene compounds. It is important to mention that the basic structure of these photoproducts represents the unsaturated structural analogues of the bicyclo[3.2.1]octane skeleton which is found in numerous biologically important active natural products.[2-5]

Our previous publications[6-13] on the photochemistry of different heteroaryl-substituted hexatrienes showed interesting intramolecular cycloaddition reactions and the formation of bicyclo[3.2.1]octadiene structures. By insertion of an additional double bond into the stilbene-like moiety, we obtained the prolonged conjugated system of **A** and **B** (Figure 1) that allowed the formation of new polycyclic structures **C** and **D** possessing the benzobicyclo[3.2.1]octadiene skeleton with the double bond functionality for further transformations (Figure 1).[1,14-17]

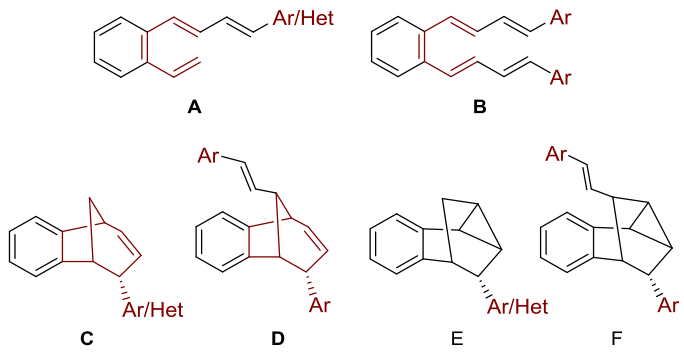

Figure 1. Starting compounds **A** and **B** in *E,E*-configuration and their photoproducts **C**-**F** (Ar/Het = phenyl, *p*-methylphenyl, *p*-chlorophenyl, *p*-methoxyphenyl, 2-furyl, 3-pyridyl, 4-pyridyl, 2-thienyl, 3-thienyl).

The starting conjugated compounds **A** and **B** undergo intramolecular photocycloaddition reaction to benzobicyclo-[3.2.1]octadiene **C** and **D**, respectively, giving only or preferably the *endo*-Ar/Het-benzobicyclo[3.2.1]octadiene isomer due to the stereoselectivity of the photoreaction. Some of the *endo*-Ar/Het-benzobicyclo[3.2.1]octadiene derivatives undergo further di-π-methane rearrangement leading to *endo*-tricyclic structures **E** and **F** (Figure 1), or they can be used as a suitable substrate for other transformations on the isolated double bond, easily derivatized to new compounds with various functionalities. Depending on the aryl or heteroaryl substituent the yields on the *endo*-Ar/Het-benzobicyclo[3.2.1]octadiene photoproducts like **C** (Figure 1) were moderate to very good (Ar/Het = phenyl (90%), *p*-chlorophenyl (77%), *p*-methoxyphenyl (55%), 2-furyl (57%), 3-pyridyl (44%), 4-pyridyl (51%), 2-thienyl (30%), 3-thienyl (37%).[1,15-17]

To get a deeper understanding of the photoinduced behavior of these conjugated systems, their spectral characterization and detailed investigation of the photochemical and photophysical behavior are examined. In these systems with prolonged conjugation, the influence of the introduced *p*-substituted aryl or heteroaryl ring is examined on the possibility of the intramolecular

[2+2]-photocycloaddition followed by the formation of the benzobicyclo[3.2.1]octadiene analogues. The possible steric hindrances probably cause deviations from planarity[18] and shift the conformer equilibrium affecting the reaction pathways and yields. As several of the conformers can react in the formation of intramolecular photoproducts, it is not expected that the photoreactions take place always from the most populated conformer regardless of the conformational distribution of the starting molecule. Although the conformers of each geometrical isomer may display deviating photoinduced behavior, similarly to some 2-vinylbiphenyls,[19] 1,2-dinaphthylethenes,[20] and 1-naphthyl-2-phenylethenes[21], investigation of the effects of the conformational diversity within the steric influence of the starting geometric isomers on the reaction pathway was not our aim in our former studies. In the study of pyridyl- and thienylbutadiene derivatives[17] it is also aimed to determine, for the first time, the efficiency of the intramolecular photocycloaddition reaction that takes place by utilizing chemical actinometry measurements.

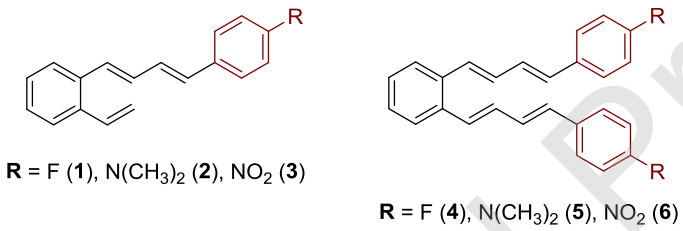

Figure 2. Structures of the investigated butadiene derivatives 1-6 in *E,E*-configuration.

In the continuation of the research, in this paper we describe our new study on photochemical and especially photophysical behavior of the butadiene derivatives where *p*-fluorophenyl, *p*-dimethylaminophenyl, and *p*-nitrophenyl rings were incorporated into the previously studied framework in mono- or di-arylbutadiene analogue (Figure 2). The deep photophysical study is performed to see the nature of photophysical processes and define competitive processes in the excited states. We predict that various electronic and steric effects of one or two different functional groups on the phenyl ring(s) in the molecule would provide a great influence on the molecular structure and photoinduced behavior. Additionally, for the first time, we performed the computational investigation of the effects of the conformational diversity within the steric influence of the starting geometric isomers on the photoreaction pathway and energy profiles of the Wittig reaction in the synthesis of **1**-**6**.

Results and Discussion

Synthesis of butadiene derivatives 1-6

Mono-arylbutadiene derivatives **1-3** and di-arylbutadiene analogues **4-6** (Figure 2) were prepared by the Wittig reaction from diphosphonium salt of α,α'-*o*-xylenedibromide and the corresponding cinnamaldehydes. The synthesis of *o*-vinyl-butadienyl derivatives **1** and **2** was utilized for the first time during the investigation of the benefits of flow photochemistry in comparison to the traditional (batch) method of related conjugated systems with diversified targeted substituents and intensification of the synthesis of benzobicyclo[3.2.l]octadiene skeleton.[22] The nitro derivative **3** was prepared at first for comparative characterization of the molecule by X-ray diffraction, analysis of crystal packings, and determining the influence of weak interactions to the crystal structure.[23] In both former works, the photophysical investigation of pure geometrical isomers of **1-3** was not in the focus of the experiments, so these results here represent the first deeper photophysical study of those mono-arylbutadienes **1-3** and additionally the new diarylbutadiene analogues **4-6** (Scheme 1).

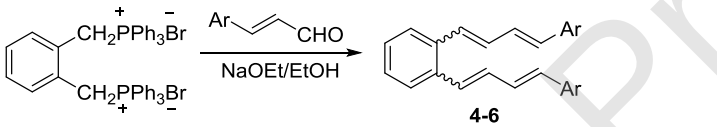

4: Ar = *p*-fluorophenyl (49%)
5: Ar = *p*-dimethylaminophenyl (64%)
6: Ar = *p*-nitrophenyl (45%)

Scheme 1. Synthesis of substituted di-arylbutadiene derivatives **4-6** by Wittig reaction.

The Wittig reaction of di-arylbutadiene derivatives **4-6** was conducted for the first time according to the "one-pot" procedure described in our previous paper[24] and gave a mixture of isomers (**4**: *Z,Z* : *E,Z* = 1:4, **5**: *E,Z* : *E,E* = 1:2 and **6**: *Z,Z* : *E,Z* = 1:1), in moderate to good yields (45-64%) (Scheme 1).

The isomers of compounds **4-6** present in the reaction mixture were isolated by column and/or thin-layer chromatography on silica gel and characterized by spectroscopic methods (see Experimental section and SI, Figures S1-S17). It is interesting to emphasize that for all three derivatives, only two geometrical isomers of three theoretically possible were detected and isolated. The nature of the fluoro, dimethylamino and nitro substituent obviously influence the formation of the preferred configuration and probably also the favourable conformation. To examine how the nature of

substituent present in the reactants influence the stereochemistry of Wittig's reactions that lead to compounds **1**-**6**, we employed DFT calculations. Mechanism of Wittig's reaction with triphenylphosphonium ylide and cinnamaldehyde is shown in Scheme 2.[25]

The energy profile for this reaction, which we calculated employing Truhlar's functional M06-2X[26] combined with 6-31+G(d) basis set, using Gaussian09 programme package,[27] is presented in Figure 3. The stationary points of reaction are localized at the potential energy surface (PES) and vibrational analysis was performed to verify the minima and transition states on the PES for all structures. The first step of the reaction, a formation of oxaphosphetane-1 (OP1), has the activation energy of 10.4 and 12.1 kcal mol^{-1} (for *E* and *Z* path, respectively), which is in agreement with previous studies.[25] This step determines the stereochemistry of the final product: transition state (TS1) forms the complex containing four-center CCOP structure where double nucleophilic addition (C to C and O to P) occurs, which leads to OP1. The inspection of the normal mode of single imaginary vibration in TS1 shows the strong interaction between the C atom of the carbonyl group and ylidic carbon, with a distance between these two atoms shortened to 2.0 and 1.9 Å for *trans* and *cis* path, respectively. This is synchronized with the mutual approaching of oxygen and phosphorus, with distance in TS1 being 3.2 and 3.6 Å (cis, trans). The described mode of vibration corresponds to the formation of the four-membered ring (CCOP) in oxaphosphetane. The frequency of imaginary vibration in TS1 is −222.3 cm^{-1} and −181.5 cm^{-1} for *trans* (*E*) and *cis* (*Z*) path, respectively.

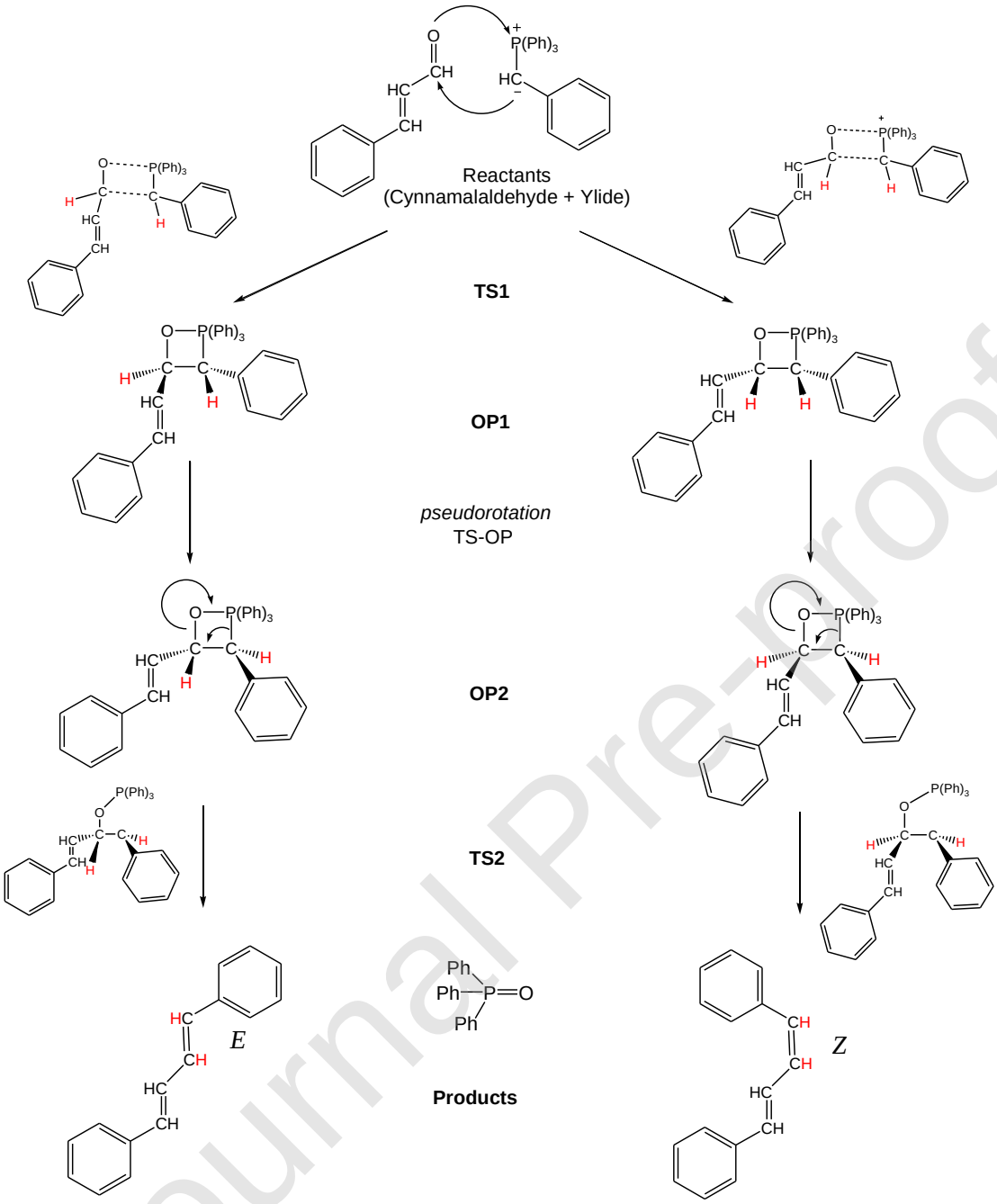

Scheme 2. Mechanism of Wittig's reaction. Left path leads to *E*-isomer, right path to *Z*.

In oxaphosphoetane-1, hydrogen at C of the carbonyl group and hydrogen at carbenium in ylide are placed either at the opposing sides of CC bond – leading to *E*-product, or at the same side of CC bond, which results in *Z*-isomer of product. Oxaphosphoetane-1 (where oxygen is in apical position) then undergoes pseudorotation and yields oxaphosphetane-2 (OP2), with ylidic carbon becoming apical. This step has been confirmed by the detection of oxaphosphetanes by low-

temperature ^{31}P NMR during reactions of semistabilized ylides.[32] The transition state for pseudorotation (TS-OP) has been located for both paths from Scheme 2, with the frequency of imaginary mode being −29.3 cm^{-1} and −32.3 cm^{-1} for *trans* (*E*) and *cis* (*Z*) path, respectively. This value is in agreement with previous computational studies of the mechanism of Wittig reaction.[25] In both paths, the calculated barrier for the pseudorotation is very low, so it is clear that this step does not play an important role in defining reactivity. Moreover, the mutual orientation of hydrogens attached to carbon atoms in CCOP does not change, so this step does not affect the stereoisomerism of the final products either. The final step is a cleavage of carbon-phosphorus bond and formation of alkene and triphenylphosphine oxide, *via* transition structure TS2.

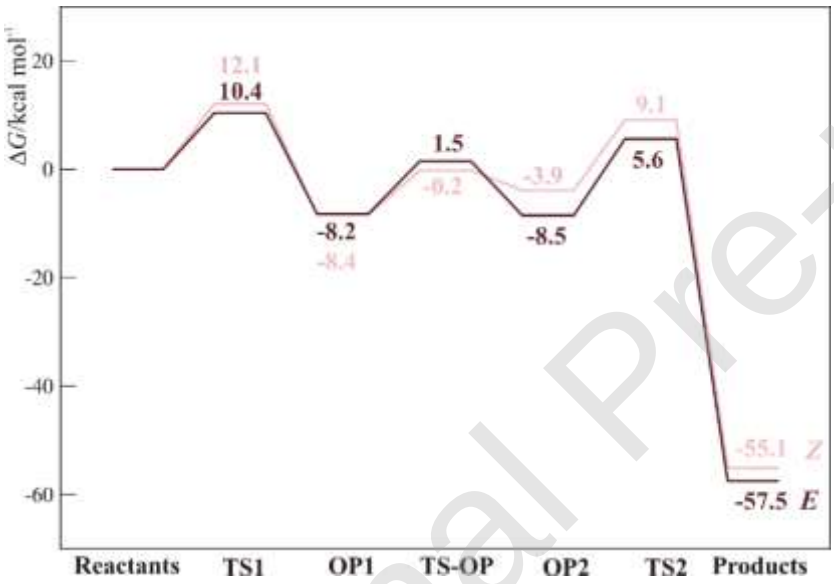

Figure 3. The free energy profile (in kcal mol^{-1}) for the reaction presented at Scheme 2, obtained at M06-2X/6-31+G(d) level of theory.

To predict how the presence of fluoro, dimethylamino, and nitro substituents influence the stereoisomerism of di-arylbutadienes **4**-**6**, we computationally investigated steps in the mechanism which determine the stereochemistry of products (i.e. formation of OP1) for these compounds. Each of these molecules contains two arylbutadiene units: first, mono-arylbutadiene is formed, using ylide that was activated by deprotonation of -CH_2 group (of -CH_2PPh_3) in the diphosphonium salt of α,α'−*o*-xylenedibromide.

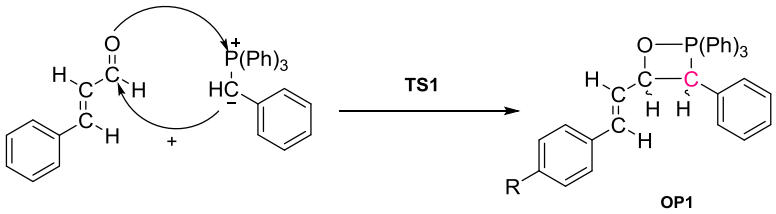

Scheme 3. Formation of oxaphosphetane-1, OP1.

After that Wittig reaction starts again by activation of the second ylide, by deprotonation of -CH_2 group placed at the ortho-position relative to the first ylide. We computed the activation energy for the formation of OP1 for the path that leads to the addition of the first arylbutadiene (Scheme 3), to estimate the stereochemistry of mono-arylbutadienes. However, the stereochemistry of the final products, di-arylbutadienes, depends on two factors: (i) isomerism of mono-arylbutadienes that has been formed in the first stage, and (ii) on the energy barrier for the formation of oxaphosphetane-1 in reaction path that leads to di-arylbutadiene (denoted here as OP1'). Therefore, the activation energy for the formation of OP1' is calculated, too (Scheme 4), and barriers for both processes are compared to estimate the stereochemistry of final products.

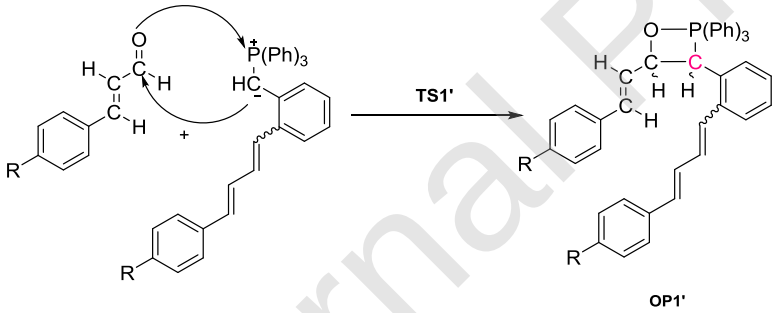

Scheme 4. Formation of oxaphosphetane-1', OP1'.

The results for R = F, $N(CH_3)_2$, and NO_2, respectively, are presented in Figure 4. In reality, the formation of TS1' does not follow directly after the formation of TS1; for the sake of convenience and simplicity, these energy barriers are presented here in a way that enables their direct comparison. Di-arylbutadiene can have *E,E*, *E,Z*, and *Z,Z*-configuration. *E,E*-product is a result of the path that goes *via* TS1 which leads to *E*-monoarylbutadiene, which is then followed by the path that goes via TS1' that gives *E* configuration of the second arylbutadiene unit. The situation is analogous for the formation of *Z,Z*-isomers. However, *E,Z*-diarylbutadiene may be formed in two

ways: *via* TS1 that leads to *E*-monoarylbutadiene and followed by the path that gives *Z*-configuration of the second arylbutadiene, and *vice versa*, *via* TS1 leading to *Z*-monoarylbutadiene, followed by the process that involves TS1' which results in *E*-configuration of the second arylbutadiene unit.

The relative barriers presented in Figure 4 show that for compound **4** (R = F) the formation of *E*-monoarylbutadiene goes faster (10.5 *vs.* 13.1 kcal mol^{-1}, similarly to unsubstituted aldehyde, Fig. 3), implying that diarylbutadienes possessing *E,E*- and *E,Z*-configuration are preferred as a final products. However, the formation of *E,E*-isomer has the highest barrier (TS1') of all (19.0 kcal mol^{-1}); therefore, in the second stage the occurence of *E,Z*-isomer is preferred. This prediction is in agreement with the experimental results: among stereoisomers of **4**, the molecule with *E,E*-configuration is not present. Formation of isomer *Z,Z*-isomer that occurs within the products is due to the lowest energy demand for the second stage, (i.e. for TS1'), however only 20% of compound **4** with *Z,Z*-configuration is present, due to the competition between *E* and *Z* path in the first stage, when the formation of TS1 that belongs to *E* path is preferred. Analogous analysis for molecule **5** (R = $N(CH_3)_2$) shows that in the first stage of synthesis, the occurrence of *E* isomer is highly preferred (12.9 *vs.* 17.8 kcal mol^{-1} for TS1 that leads to *E* and *Z*-monoarylbutadiene, respectively.

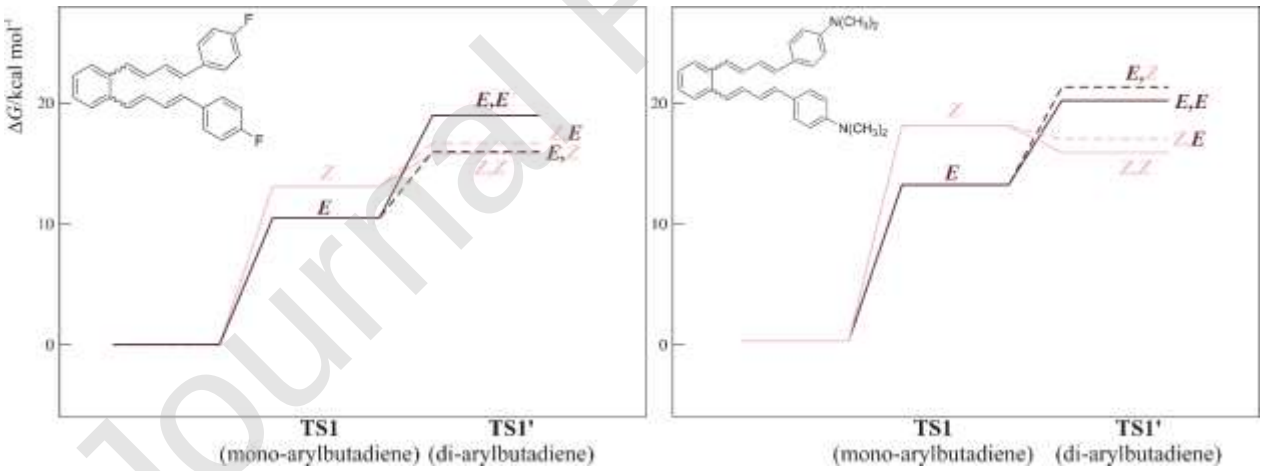

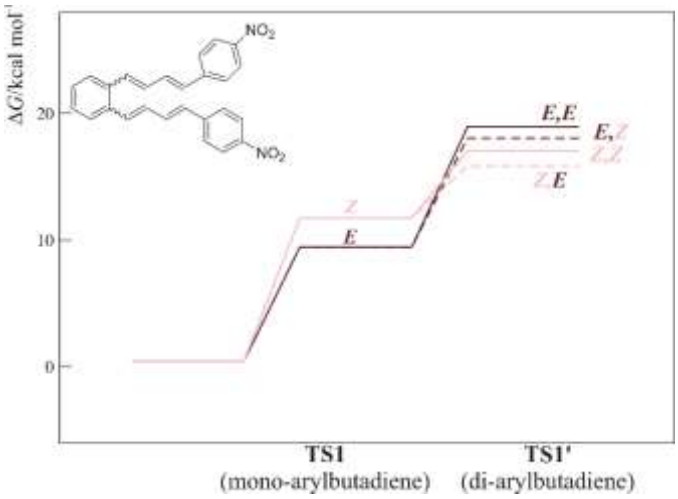

Figure 4. Direct comparison of calculated free energy barriers for the formation of OP1, and OP1', that lead to mono-arylbutadiene and diarylbutadiene, for molecules **4**, **5**, and **6**.

Therefore, among the final products of **5**, isomers *E,E,* and *E,Z* dominate, whereas the *Z,Z* is not present at all despite the barrier for TS1' being the lowest – there is no *Z*-monoarylbutadiene to enable the formation of *Z,Z*-diarylbutadiene. In molecule **6**, the barriers for *E* and *Z* are similar and competitive (11.3 and 9.0 kcal mol^{-1}), implying that both *E* and *Z*-monoarylbutadiene occur in the first stage, but the formation of *E,E*-diarylbutadiene here is not probable, since the energy barrier for this path is the highest (18.3 kcal mol^{-1}). These predictions for molecules **5** and **6** are also in agreement with experimental results.

To summarize these findings, for compounds **4** and **6**, the first phase of synthesis gives both (*Z* and *E*) stereoisomers of mono-arylbutadiene, so the stereochemistry of the final product is determined by the second phase, during the formation of TS1'. However, for dimethylamino-substituted compound **5**, the stereochemistry of the final product is already defined in the first phase, when path leading to *E* stereoisomer of mono-arylbutadiene is highly preferred.

Preparative photochemistry of compounds 1-6

The preparative irradiation experiments were performed in toluene solutions under anaerobic conditions at 350 nm and low concentrations in the order of 10^{-3} M suitable for intramolecular reactions. The systems were argon-saturated to avoid the photoinduced oxidation of the excited molecules. Depending on the starting material and different substituents, various photochemical routes were identified and confirmed. The formation of the photoproducts was generally accompanied by the formation of some polymeric products which are not further investigated.

The photochemistry of *o*-vinyl-butadienyl derivatives **1**-**3** was utilized for the first time during the investigation of flow photochemistry and targeted cycloaddition to benzobicyclo-[3.2.l]octadiene skeleton[22] but no attempt was made to investigate the deeper photochemical or photophysical behavior of isolated isomers and/or deactivation processes.

Utilizing the stereoselective intramolecular cycloaddition of **1**-**6** by flow photochemical approach, we obtained the desired structures of the photoproducts (Figure 5) in the case of starting mono-*p*-fluorophenyl-butadiene **1** (87% isolated yield of *endo*-**7**) and di-*p*-fluorophenyl-dibutadiene **4** (36% isolated yield of *exo,endo,trans*-**9**) both with complete consumption of starting material, respectively, and in 24% of isolated yield for *endo*-**8** in the case of starting substrate mono-*p*-dimethylamino derivative **2**, with 60% of consumption. Obviously, the tertiary amino group in the photoproduct *endo*-**8** (in comparison to photocycloadducts *endo*-**7** and *exo,endo,trans*-**9** with one or two fluoro substituent(s)) contributes to the lower stability possibly through the lowering of the intensity of π–π interactions by competitive electronic effects. Evidently, the strong electronic effects of the *p*-dimethylamino in the starting substrate **2** during the photocycloaddition reaction also bring to the incomplete consumption of the starting material. With this double effect, the result of photochemistry of the derivative **5** with two *p*-dimethylamino groups in the starting structure did not give any photoproduct. Starting compound **4** gave also one minor polycyclic photoproduct *endo,trans*-**10** in 18% of isolated yield (Figure 5). In the case of compounds **1** and **2**, only in traces, tricyclic structure like **E** (Figure 1) can be detected from the NMR spectra of the photomixture due to characteristic signals in the aliphatic region. Nitro derivatives **3** and **6** show photochemical unreactivity and no formation of any cycloadduct.

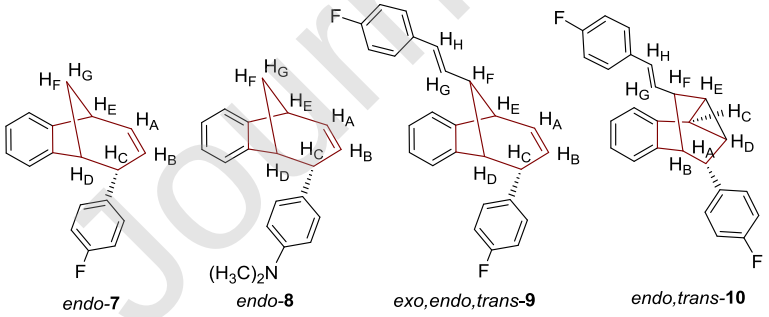

Figure 5. Structure of fluoro- and dimethylamino-substituted photoproducts *endo*-**7**, *endo*-**8**, *exo,endo,trans*-**9** and *endo,trans*-**10** with proton assignments (A-G or A-H).

In the case of **4**, intramolecular cycloaddition reaction is the favorable photochemical path giving, besides *exo,endo,trans*-**9**, the other stereoisomer *endo,endo*-**9** in traces. The formation of **9** is

explained by the same mechanism (Scheme 5) as described for related derivatives in one of our previous papers[1,14,22] from the preferred conformation of *trans,trans*-**4** *via* a 1,4-biradical **11** followed by the preferred cyclohexene ring closure to product **9**.

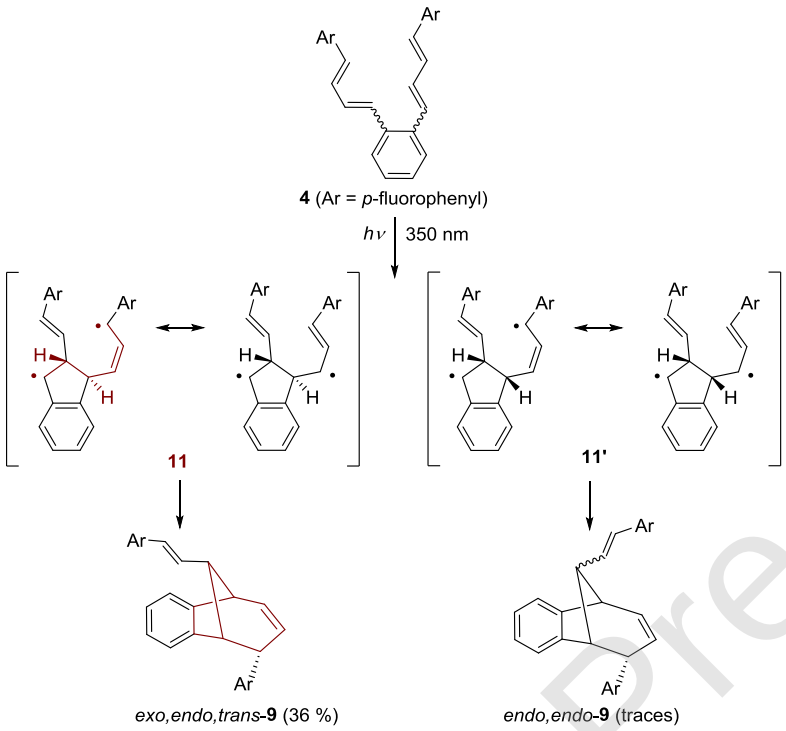

Scheme 5. Proposed mechanism for the formation of the benzobicyclo-[3.2.1]octadiene structure *endo,endo,trans*-**9** from *p*-fluoro substituted derivative **4**.

The preferred ring closure with endo-orientation of one *p*-fluoro-phenyl group can be ascribed to the stabilization of the transition state by the strong attractive intramolecular π–π interactions of the benzo-phenyl groups.[28-30]

The stereoselective formation of exactly the *exo,endo,trans*-**9** with the *exo*-orientation of the unreacted styryl group can be explained (Scheme 5) by preferred trans ring closure to the indane intermediate **11**, presumably because of steric reasons, which then closes to yield *exo,endo,trans*-**9**. The formation of the *endo,endo*-isomer, found only in traces, was explained by cis ring closure to the indane intermediate **11'**. The proposed mechanism (Scheme 2) suggests the formation of the intermediate **11** from the *trans,trans*-**4**, which is in accordance with the photophysics showing that the all-trans configuration of **4** contributes the most to the relaxation *via* photochemical and internal conversion processes. After the complete conversion, the exact main photoproduct *exo,endo,trans*-

9 was separated and isolated by column chromatography on silica gel, and its structure was deduced unequivocally from spectral studies (see Experimental section and SI, Figures S18-S23). The formation of benzotricyclic compound *endo,trans*-**10** from the starting compound **4** at 350 nm could be explained (Scheme 6) only by initial sixmembered-ring-closure *via* **12** and consequent thermal [4+2]-cycloaddition and re-aromatisation. The preferred *endo*-orientation of one *p*-fluoro-phenyl group and *trans*-configuration on the double bond are explained and confirmed as in the case of *exo,endo,trans*-**9**.

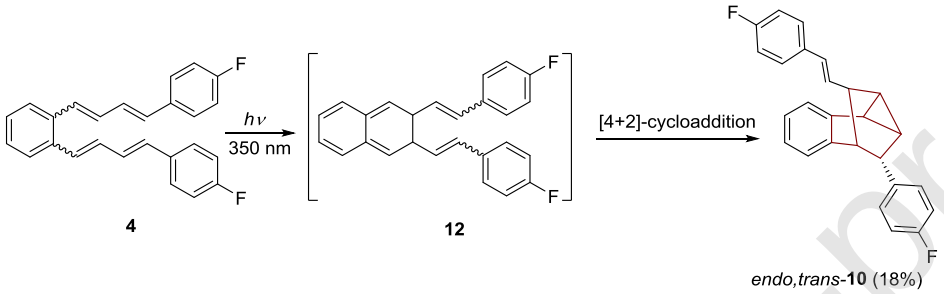

Scheme 6. Proposed mechanism for the formation of the tricyclo structure *endo,trans*-**10** from *p*-fluoro-substituted derivative **4**.

From the NMR spectra of *exo,endo,trans*-**9**, using additional techniques (COSY and NOESY) the structure was completely assigned. It can be seen the resolved four-proton pattern in the ^{1}H NMR spectrum (Figure 6) between 3.2 and 4.1 ppm unmistakably points to the bicyclo[3.2.1]octadiene structure. The *exo*-orientation of the styryl at the methano bridge carbon is defined on the basis of COSY interaction between protons F and G (Figure 6).

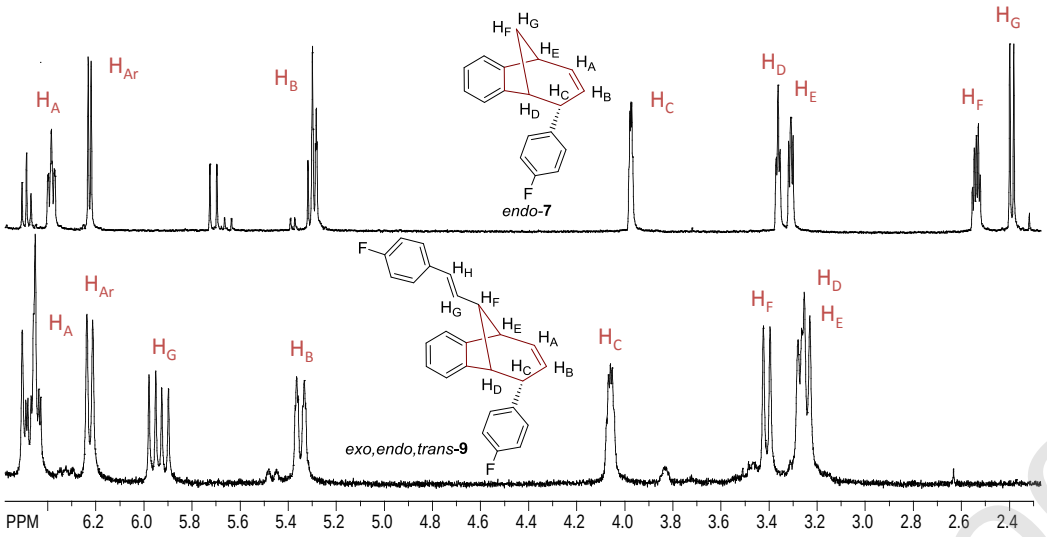

Figure 6. The crucial part of the ^{1}H NMR spectra of *endo*-**7**[22]; and *exo*,*endo*,*trans*-**9** ($CDCl_3$, 300 MHz).

In previously obtained bicyclo[3.2.1]octadiene derivatives[1,22] with no substituent on the methano bridge carbon, the proton F couples only with the *exo*-oriented proton G. As the *endo*-oriented proton does not couple with the proton F, the *exo*-structure was assigned. The *trans*-configuration on the styryl substituent on the methano bridge is confirmed by the existence of two coupling constants with 16.1 Hz for protons G and H (see Experimental section and SI, Figures S21-S22). The signals in the lower field between 5.3 and 6.5 ppm are assigned to the A and B protons on the isolated double bond. One of the aromatic protons, H_{ar} of the benzo moiety is shifted to the higher field at 6.2 ppm due to the anisotropic effect of phenyl *endo*-substituent.

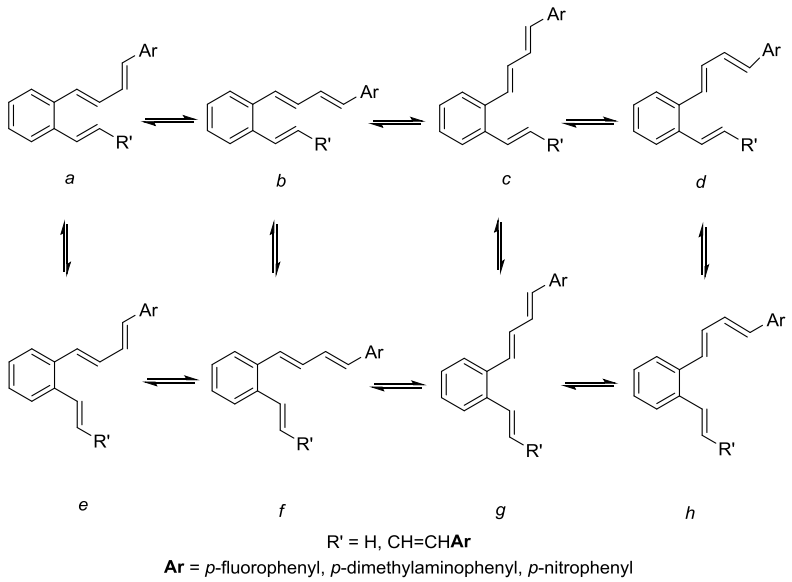

Scheme 7. Possible conformations of *E*-isomers of **1-3** and *E,E*-isomers of **4-6**.

Conformational analysis of compounds **1-6** is performed using the M06-2X/6-31G(d,p) level of theory. Conformers of *E*-isomers of **1-3** and *E,E*-isomers of **4-6** (that further go to the productive photochemical reactions) are shown at Scheme 7. Figure 7 shows the relative stabilities of conformers for molecules **1-6**. Relative stability ΔG^{298} (in kcal mol^{-1}) is obtained as a difference between computed Gibbs energy of each examined conformer and the most stable one found for each compound **1-6**.

For all systems, the most stable conformation is the one denoted as *g* (Scheme 7), which was expected, because it is clear that this structure has the least steric hindrance (Figure 8). The overall conclusion is that there is no big diversity in relative stabilities of conformers within compounds with different substituents: for both series, mono- (**1-3**) and di-arylbutadienes (**4-6**), the sequence of first three most stable conformations is the same (*g*, *f*, *c*), with the difference in stability not larger than 2 kcal mol^{-1}. The least stable conformation in all systems is conformer denoted as *a*, with ΔG values going from 6.4 to 8.1 kcal mol^{-1} (see SI, Table S1). The remaining four conformers (*b*, *d*, *e*, *h*) in all molecules have relatively close values of energy, with deviation from the most stable conformer between 2.5 and 4.8 kcal mol^{-1}.

Although butadiene derivatives **3** and **6**, which contain nitro substituent, do not undergo photochemical synthesis, their conformations were analyzed to see if the electron-withdrawing

group such as $–NO_2$ has any effect to the relative stabilities of conformers compared to derivatives with electron-donating substituent (dimethylamino group).

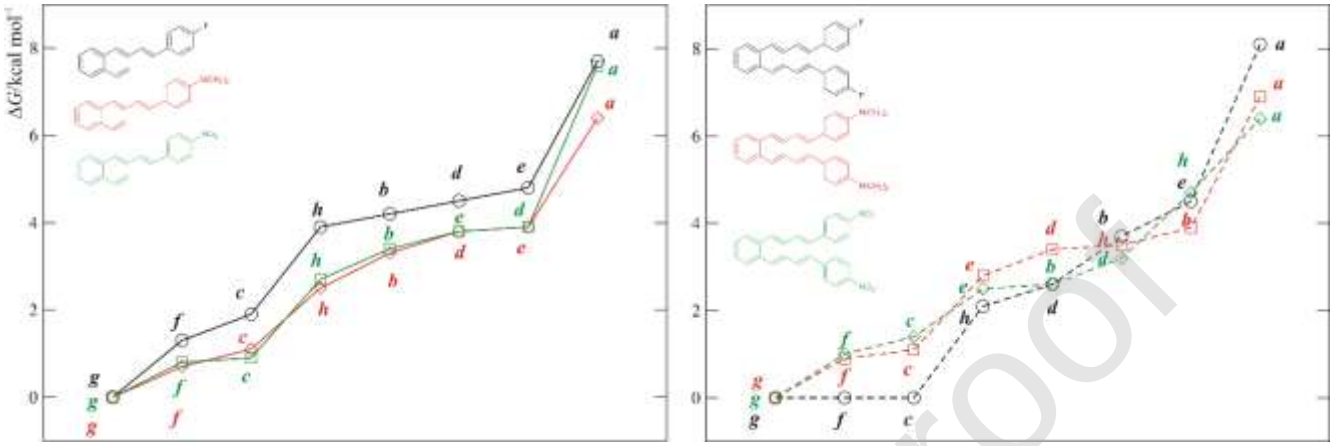

Figure 7. Stabilities of conformers of molecules **1-3** (left) and **4-6** (right), calculated as Gibbs energies relative to the most stable conformer for each compound (in kcal mol^{-1}

The electron-inductive effect of substituents placed in the *p*-position of phenyl in studied systems did not make any significant influence on the energy distribution of conformers of isomers that are relevant for further photochemical synthesis.

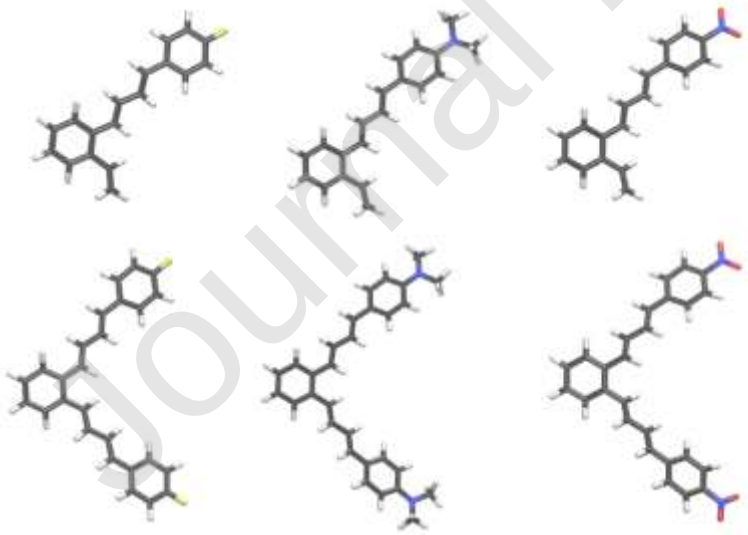

Figure 8. The structures of the most stable conformer for molecules **1-6**, optimized at M06-2X/6-31G(d,p) level of theory.

Absorption and emission spectra of compounds with one butadiene chain 1-3

Absorption spectra of 1-3. The UV spectra of separated *cis*- and *trans*-**1**, **2**, and **3**, respectively (Figures 9-11)**,** clearly indicate that the absorption characteristics considerably depends on the (*cis-trans*) configuration, on the substituents in *para* position on the phenyl group, and (in the case of the nitro-substituted derivatives) on the solvent as well. Interestingly, in the case of **1** (with fluoro substituent), the spectra in ethanol well agree with those of the corresponding unsubstituted analogues.[1] This phenomenon suggests that, despite the high electronegativity of fluorine, it does not influence the energy levels of the electronic states involved in the UV spectra of these compounds. It may be the result of two opposite effects counterbalancing each other. Accordingly, mesomer (resonance) and inductive effects may result in such an extinction. Notably, the spectra of the corresponding compounds having thiophene instead of phenyl group at the end of the butadiene chain[17] display spectra in ethanol with characteristics very similar to those of the phenyl derivatives.

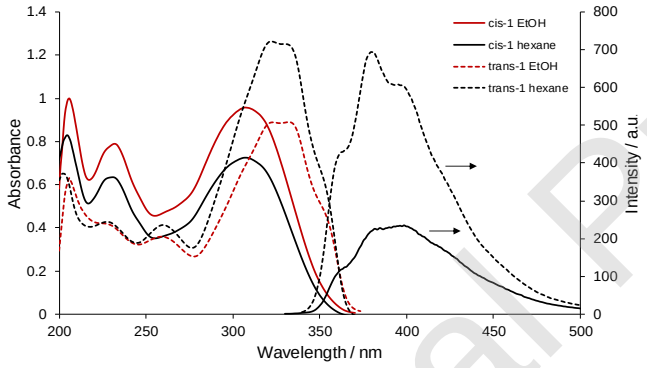

Figure 9. Absorption and emission spectra of the isomers of compound 1 in EtOH (red) and *n*-hexane.

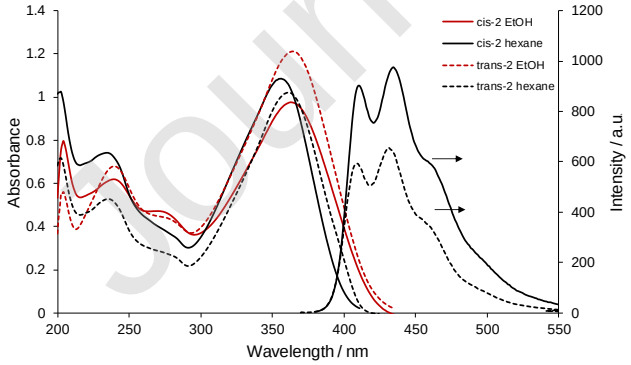

Figure 10. Absorption and emission spectra of the isomers of compound **2** in EtOH (red) and *n*-hexane.

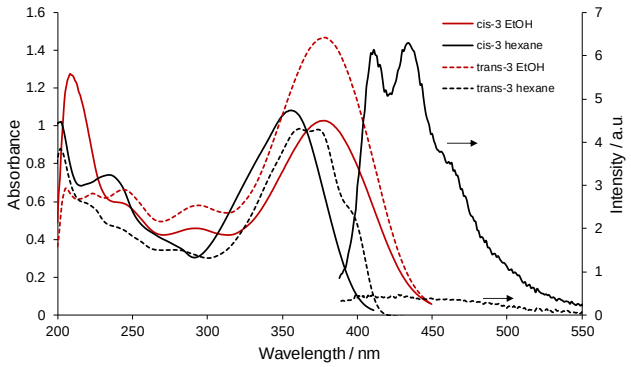

Figure 11. Absorption and emission spectra of the isomers of compound **3** in EtOH (red) and *n*-hexane.

Similarly to the unsubstituted phenyl derivatives,[1] the *cis* isomer of **1** displays a characteristic wide band at 306-308 nm in both ethanol and *n*-hexane, while the corresponding *trans* species exhibits a double band with maxima at 322 and 335 nm. This deviation may be attributed to the structural difference affecting the conjugation of the double bonds. The *cis* arrangement is less favorable in this respect, hence the weaker conjugation results in a higher energy difference between the (π and π^*) orbitals involved in the corresponding transitions. Besides, the double band indicates the appearance of the vibrational fine structure of the electronic transition, which is generally the consequence of a weaker interaction between the solvent and the dissolved compound. Accordingly, the *trans* configuration of **1** decreases the interaction with both of these solvents. In the case of the nitro-substituted derivatives, both *cis*- and *trans*-**3**, the appearance of the vibrational fine structure in *n*-hexane suggests that nitro group results in a relatively high dipole moment in the excited state. Hence, the much stronger interaction with a more polar solvent such as ethanol completely vanishes the fine structure of the absorption band as also observed earlier in the case of nitro-substituted 2,3-distyrylfurans.[31] The least influence of the *cis-trans* configuration on the absorption spectrum was observed for the dimethylamino-substituted derivatives, *cis*- and *trans*-**2**. Their spectra were very similar, displaying a strong band at about 364-367 nm in ethanol, without any vibrational fine structure, which may be attributed to the strong interaction *via* hydrogen bonds between EtOH and the amino groups. Only a very moderate red shift could be detected in the case of the *trans* configuration compared to the *cis* one (360 nm *vs.* 364 nm). This suggests a stronger conjugation of the double bonds in the former isomer, which is in accordance with the observation at the fluoro derivatives (*cis*- and *trans*-**1**). In *n*-hexane, both isomers displayed a slight blue shift of this band compared to its wavelength in ethanol. This phenomenon

suggests a moderate increase of the dipole moment in the excited state compared to the ground state.

Emission spectra of 1-3. Some characteristic features of the emission spectra (also accompanied by the excitation spectra corresponding to the absorption spectra) will be shown here. Besides, what more important is, generally, the quantum efficiency of the emission (fluorescence) is orders of magnitude lower than the primary photochemical quantum yield for each compound studied, in accordance with the high efficiency of the latter one (see in Table 1). Since the preliminary experiments indicated that EtOH as solvent displayed own emissions very disturbing those of the butadiene derivatives, regarding both the spectral characteristics and the lifetime of the their luminescence, only solutions in n-hexane were used for these measurements. It is was reasonable for the comparisons with the luminescence properties of the analogous compounds with double butadiene structure, due to their very limited solubility in EtOH. Regarding the lifetime of the emissions displayed by all compounds studied, it did not exceed 0.1 ns, the lower limit for our equipment. This observation, on the basis of the results regarding compounds with similar structures, predicted rather low quantum efficiencies for the butadiene derivatives studied in this work.

Upon excitation at 313 nm, *cis*-**1** displayed characteristic fluorescence with the main band at 399 nm, merged with a less intense one at 384 nm and a shoulder at 363 nm (Figure 9). The emission spectrum of the corresponding trans isomer displayed a much better resolved fine structure, in which the shorter-wavelength shoulder in the previous case became a distinct band at 363 nm, while the most intense peak arose at 379 nm. This phenomenon is in a good accordance with the characteristics of the corresponding absorption spectra, due to the stronger conjugation and weaker interaction with the solvent in the case of the trans configuration.

The resolutions of the corresponding bands in the emission spectra of the cis and trans isomers of the dimethlyamine-substituted derivatives (**2**) are more similar (Figure 10) than for those with fluoro groups (1). For *cis*-**2**, the main band arose at 437 nm, merged with a less intense one at 412 nm and a shoulder at 462 nm. The corresponding wavelengths for *trans*-**2** are 433, 411, and 459 nm. These values indicate moderate blue shifts in each cases. This phenomenon, suggests that the structure of the trans isomer, due to the enhanced conjugation, is more rigid as confirmed by the moderately lower Stokes-shift compared to that of the *cis* configuration (337 cm-1 *vs.* 374 cm-1).

For the nitro-substituted *cis*-**3** isomer, two separated bands, at 412 and 435 nm, can be observed in the emission spectrum, along with a shoulder at 463 nm (Figure 11). Compared to the spectrum of the corresponding fluoro derivative (*cis*-**1**), a significant red shift can be observed at each wavelength, while the spectrum of the dimethlyamino analogue (*cis*-**2**) is very similar to that of *cis*-**3**. These relations can be accounted for the electronic effects of these substituents. Unfortunately, the emission of *trans*-**3** in *n*-hexane was extremely weak, hence its spectrum could not be reliably characterized.

Photolysis of monoarylbutadienyl derivatives 1-3

The photolysis of *cis*- and *trans*-**1**, **2**, and **3** compounds at wavelengths corresponding to the main absorption bands (313 nm for **1** and 365 nm for **2** and **3**) generally resulted in a rather fast isomerization as the primary photochemical reaction. In this respect, the fluoro-substituted derivatives displayed the most characteristic spectral changes in ethanol (Figures 12a and 13a).

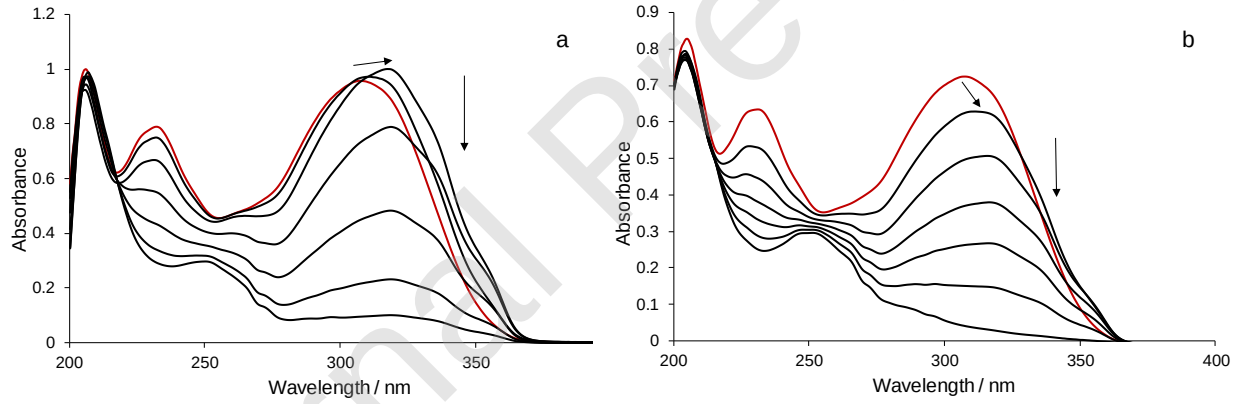

Figure 12. Spectral change during the irradiation of *cis*-**1** in EtOH (a) after 0 (red), 105, 525, 2685, 9285, 12885 s; and in *n*-hexane (b) after 0 (red), 40, 80, 120, 160, 220, 520 s (λ_{ir} = 313 nm, l = 1 cm).

No matter, which isomer is the starting compound of the photolysis, the resulting spectrum of the product(s) of the primary photochemical reaction was the same, and it unambiguously differed from those of both starting compounds. It is red-shifted compared to the main band of *cis* -**1**, while blue-shifted in relation with that of the *trans*-**1** isomer, displaying the maximum at about 321 nm. Besides, its characteristics indicate a slight vibrational fine structure by the appearance of shoulders on both sides. It suggests that its interaction with ethanol is weaker than that of the *cis*-isomer, but

stronger than that of the *trans* one. From the four isomers of **1**, both starting compounds (*cis*- and *trans*-**1**) contain *trans* configuration at the double bond connecting to the fluoro-substituted phenyl group. Hence, as the other two isomers (containing *cis*-configuration at that double bond) could come into consideration. Theoretically, both could be formed upon excitation, however, as it was discussed in the interpretation of the absorption spectra, *cis* configuration is less favorable for the conjugation, increasing the energy difference between the (π and π^*) orbitals involved in the corresponding transition. Hence, the main band of this isomer would display a blue shift compared to that of *cis*-**1**. Thus, the other possible isomer is a more reasonable candidate as a product of the photoisomerization in the respects of both the position and the fine structure of the main band. Notably, the corresponding unsubstituted analogues behaved very similarly upon irradiation in ethanol,[1] indicating that not only the spectra but the primary photoreactions of these two types of derivatives agree very well.

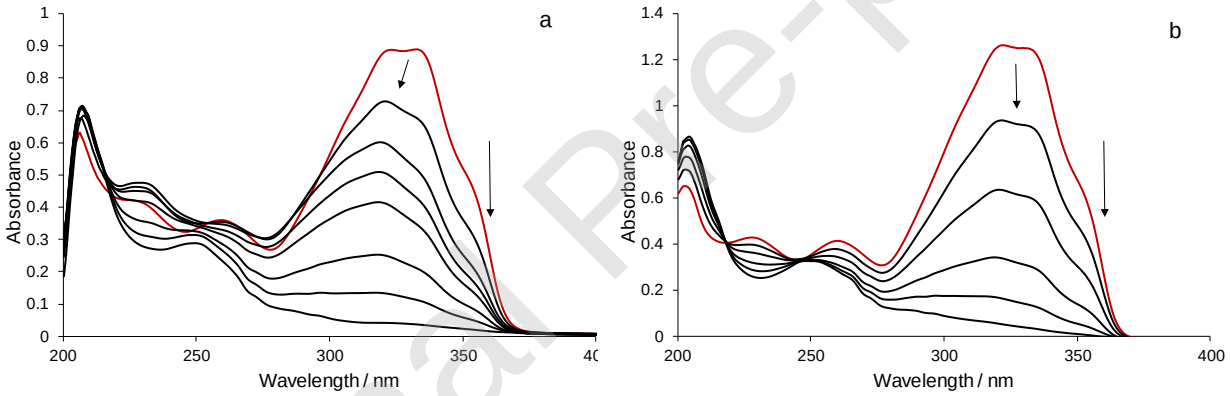

Figure 13. Spectral change during the irradiation of *trans*-**1** in EtOH (a) after 0 (red), 20, 80, 180, 320, 640, 1060, 4000 s; and in *n*-hexane (b) after 0 (red), 30, 70, 130, 210, 570 s (λ_{ir} = 313 nm, l = 1 cm).

The photoisomerization took place within less than 10 minutes for *cis*-**1** in ethanol (Figure 12a), and its quantum yield determined from the initial rate of the reaction was rather high (0.26). It is in accordance with the very low value of the fluorescence quantum efficiency (see above). Nevertheless, competitive photophysical (or –chemical) processes may take place such as internal conversion, intersystem crossing, or another transformation.

After the isomerization, the excitation of the photoisomer led to a rather fast transformation accompanied by the disappearance of the main (longer-wavelength) band at 321 nm, indicating

the ceasing of the conjugation. This is in accordance with the result of the preparative photochemistry. The quantum yield of this transition in ethanol was rather low (0.015). Notably, in *n*-hexane the corresponding quantum yields were considerably higher than those in ethanol; 0.94 for the isomerization and 0.43 for the transformation. These are in accordance with the 87% yield of the *endo*-**7** photoproduct at complete consumption of the starting compound in the preparative photolysis.

The spectral changes of *cis*- and *trans*-**1** during the photolyses in *n*-hexane are shown in Figures 12b and 13b, respectively. The corresponding quantum yields are involved in Table 1. The higher quantum yields in *n*-hexane indicate that the intermediate and the final product are better stabilized in this apolar solvent than in ethanol.

Table 1. Absorption and emission parameters as well as photochemical quantum yields of butadiene derivatives at room temperature.

compound (solvent)	λ_{abs}, nm[a]	λ_F, nm[a]	Stokes-shift cm^{-1}	Φ_F (λ_{exc}, nm)[b]	Φ_{iso} (λ_{ir}, nm)[b]	Φ_p (λ_{ir}, nm)[b]
cis-**1** (EtOH)	306				0.262 (313)	0.015 (313)
(*n*-hexane)	308	363[sh], 384, 399	492	0.028 (313)	0.939 (313)	0.426 (313)
trans-**1** (EtOH)	322, 335				0.743 (313)	0.076 (313)
(*n*-hexane)	322, 333	363, 379, 399	248	0.111 (335)	≈0.85(313)	<0.85 (313)
cis-**2** (EtOH)	360				<1 (366)	0.020 (366)
(*n*-hexane)	357	412, 437, 462[sh]	374	0.076 (367)	0.914 (366)	0.095 (366)
trans-**2** (EtOH)	364				0.885 (366)	0.011 (366)
(*n*-hexane)	361	411, 433, 459[sh]	337	0.103 (367)	0.916 (366)	0.049 (366)
cis-**3** (EtOH)	378				<1 (366)	0.0022 (366)
(*n*-hexane)	351	412, 435, 463[sh]	422	0.0011 (360)	<1 (366)	0.0051 (366)
trans-**3** (EtOH)	378				0.034 (366)	0.0006 (366)
(*n*-hexane)	361, 376, 399[sh]	≈ 420 (very weak)	125	0.0001 (360)	<1 (366)	0.0013 (366)
cis,cis-**4** (*n*-hexane)	290, 327	361[sh], 385, 405, 426[sh]	288	0.0063 (324)	-[c]	-[c]
cis,trans-**4** (*n*-hexane)	355, 390[d], 411[sh]	437[sh], 462	145	0.0043 (353)	-[c]	-[c]
cis,trans-**5** (*n*-hexane)	356, 382	437, 463, 490[sh]	329	0.0077 (352)	0.890 (366)	0.0022 (366)
trans,trans-**5** (*n*-hexane)	354, 383	435, 463	312	0.0049 (355)	0.736 (366)	0.0027 (366)
cis,cis-**6** (*n*-hexane)	306, 340	360, 376, 394	163	0.0018 (313)	0.125 (336)	0.0049 (366)

[a]The main maximum is underlined. [b]Standard deviation ±5%. [c]Not measurable. [d]Approached by the excitation spectrum.

Also the primary photoisomerization of the dimethylamine-substituted derivatives (*cis*- and *trans*-**2**) was very fast (Figure 14 and 15), the quantum yield for this step was close to unity for these isomers in both EtOH and *n*-hexane. The isomerization was accompanied by a slight red shift in

the case of *cis*-**2** in both solvents, while no shift of the main band occurred for the *trans* isomer, leading to the formation of a common photoisomerization product from both starting compounds.

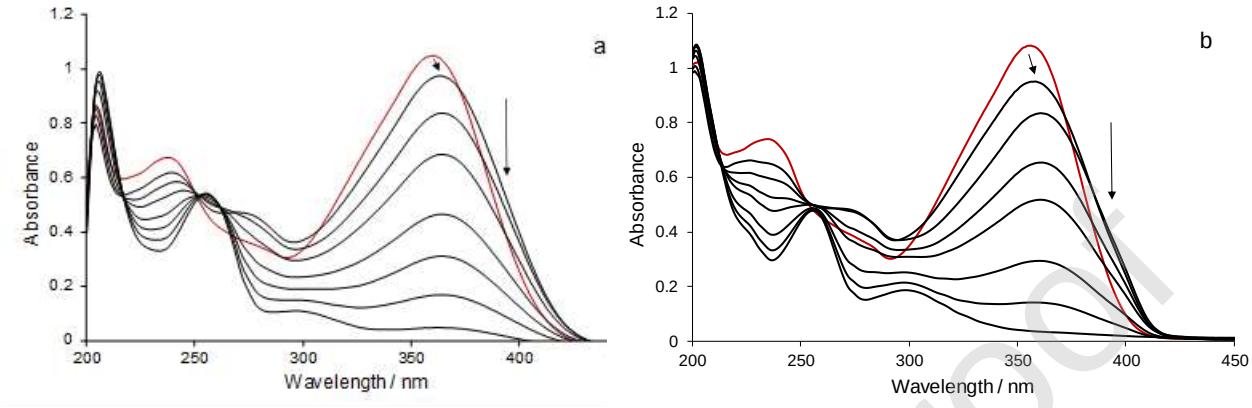

Figure 14. Spectral change during the irradiation of *cis*-**2** in EtOH (a) after 0 (red), 30, 570, 1230, 1890, 2670, 3990, 5670 s; and in *n*-hexane (b) after 0 (red), 30, 180, 390, 570, 930, 1350, 2370 s (λ_{ir} = 366 nm, l = 1 cm).

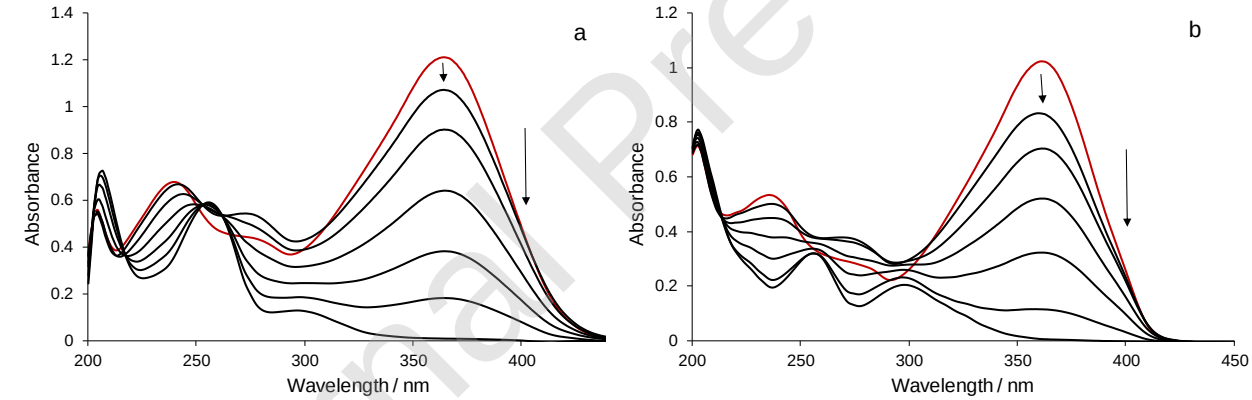

Figure 15. Spectral change during the irradiation of *trans*-**2** in EtOH (a) after 0 (red), 30, 690, 1770, 3090, 4530, 9210 s; and in *n*-hexane (b) after 0 (red), 40, 300, 700, 1240, 2200, 4720 s (λ_{ir} = 366 nm, l = 1 cm).

This, similarly to the case of the fluoro-substituted derivatives, contains cis configuration regarding the double bond closer to the dimethylamine-substituted phenyl group. (Notably, the spectrum of this isomer was very similar to that of *cis*-**2**, but the fast change of the absorption in the first minute of the irradiation clearly indicated the photoisomerization.) However, the transformation of the photoisomer was considerably slower than in the case of **1**. The quantum yields in *n*-hexane were in the range of 0.05-0.10. (In EtOH, similarly to the fluoro-substituted derivatives, the quantum

yields for the transition of the photoisomer(s) were much lower than those in *n*-hexane, in the range of 0.011-0.020.) This lower reactivity of the dimethylamine-substituted derivatives may be attributed to the enhanced stability due to the conjugation strengthened by the $N(CH_3)_2$ group, from which the donation of the lone pair is promoted by the two alkyl groups. This diminished reactivity is in accordance with the lower yield (36%) of the *endo*-**8** photoproduct in the preparative photolysis with the incomplete (60%) conversion of the starting compound.

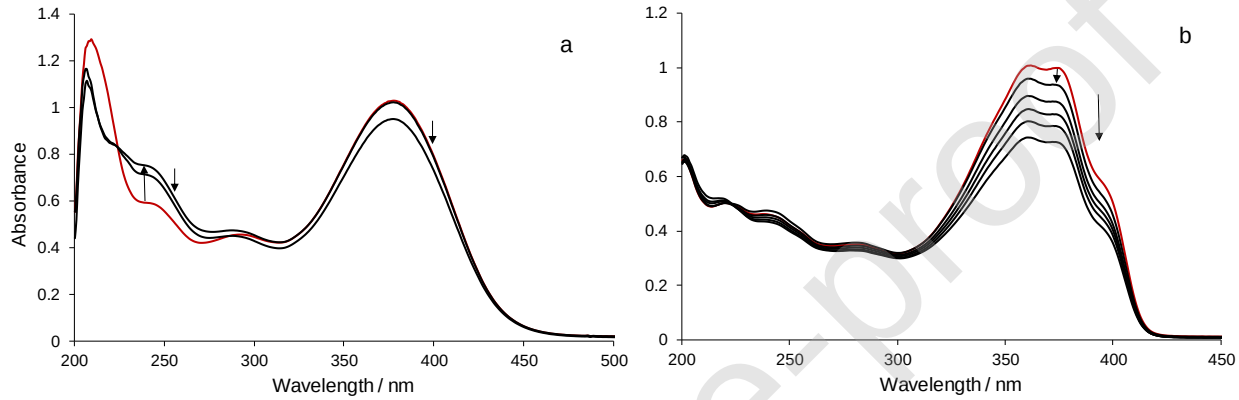

Figure 16. Spectral change during the irradiation of *cis*-**3** in EtOH (a) after 0 (red), 450, 8550 s; and in *n*-hexane (b) after 0 (red), 30, 2970, 6150, 9030, 13500 s (λ_{ir} = 366 nm, l = 1 cm).

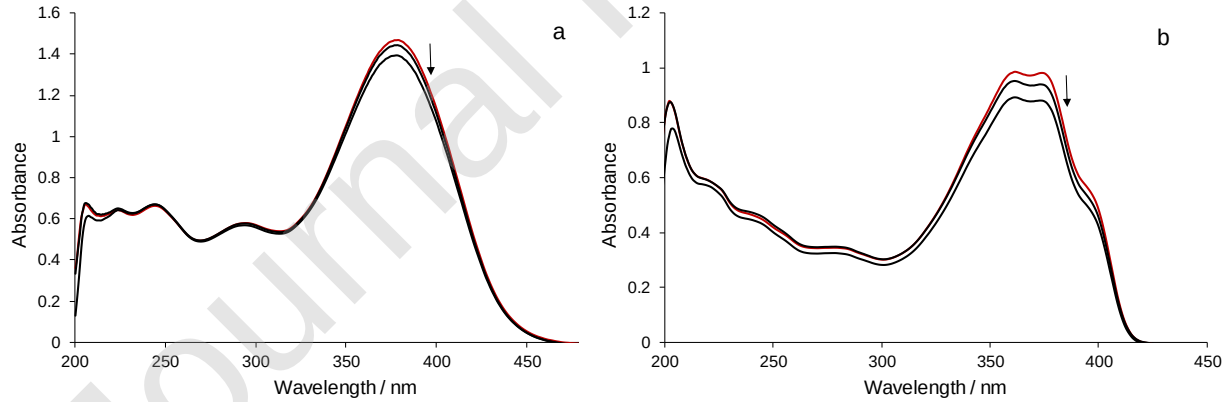

Figure 17. Spectral change during the irradiation of *trans*-**3** in EtOH (a) after 0 (red), 570, 7230 s; and in *n*-hexane (b) after 0 (red), 90, 7470 s (λ_{ir} = 366 nm, l = 1 cm).

The nitro-substituted derivatives (*cis*- and *trans*-**3**) behaved similarly to the dimethylamine-substituted analogues, but with an even lower reactivity after photoisomerization (Figure 16 and 17). In *n*-hexane, the photoisomerization is very fast for both starting isomers of **3**, taking mostly place in the first one minute (see Figure S24), with a quantum yield about unity (Table 1).

Subsequently, the transition of the photo-isomer(s) was extremely slow, with quantum yields in the range of 0.001-0.006 (one order of magnitude lower than those for the dimethylamine-substituted derivatives). In EtOH the photoinduced behavior of *cis*-**3** well agreed with that in *n*-hexane, with about the same quantum yields. Interestingly, in the case of *trans*-**3** the primary photoisomerization step was rather slow (with a quantum yield of 0.034), hence no breaking point could be observed in the absorption change at the transition from the isomerization to transformation (Figure S25). The very low quantum yield of the latter reaction for the nitro derivatives is in good accordance with the lack of any photocycloadduct in the preparative photolysis. This unreactivity may be attributed to the strong electron-withdrawing effect of the NO_2 group. This substituent in *para*-position considerably decreases the electron density on the conjugated double bond system, reducing the chance for the photocycloaddition, the determining reaction in the preparative photolysis. A similar phenomenon was observed for the nitro-substituted 2,3-distyrylfurans.[29]

Absorption and emission spectra of compounds with two butadiene chains 4-6

As to the compounds with two butadiene chains, their solubilities in *n*-hexane, and especially in EtOH are rather limited. Hence, they were only studied in the less polar solvent. Even so, one of the six compounds proved to be insoluble in *n*-hexane, and two others could only be dissolved in a very low concentration, which made luminescence measurements possible. These concentrations were not enough for reliable photolysis experiments (with quantum yield determinations), but the characteristic spectral changes upon irradiations could be detected.

Absorption spectra of 4-6

Unfortunately, the fluoro derivatives of the compounds with two butadiene chains (*cis,cis*- and *cis,trans*-**4**) could only be dissolved in very low concentrations. Hence, the absorption spectrum of the *cis,cis*-configuration is a bit uncertain, while in the case of the *cis,trans* isomer-only the excitation spectrum can be used for the approach of the absorption characteristics. Nevertheless, also these possibilities could be used for the detection of the effects of the substituent and configuration.

The absorption spectrum of the *cis,cis*-**4 i**somer displays a strong band at 290 nm, partly merged with another band at about 327 nm (Figure 18). The excitation spectrum of the *cis,trans*-isomer also displays two bands in the 250-400-nm range (at 359 and 397 nm), but more separated than in

the case of the *cis,cis*-configuration. These values clearly indicate that the energies for the corresponding transitions in the *trans*-configuration are significantly lower than those in the *cis* one. A similar phenomenon was observed for the derivatives with one butadiene chain and can be attributed to the stronger conjugation in the trans conformation, leading also to a more planar structure.

In the case of the dimethylamine-substituted derivatives (**5**), the *cis,trans*- and *trans,trans*-isomers were investigated. Similarly to the analogues with one butadiene chain, the configuration hardly affects the absorption characteristics. Both isomers display two bands; at about 354-356 nm and 382-383 nm (Figure 19). This phenomenon indicates that the dimethylamine substituents, due to their efficient lone pair donating feature, so strongly stabilize the electronic structure of the conjugated system that not even the configurational change can significantly influence the energy differences of the states involved the corresponding transitions.

This is in accordance with the low reactivity for photo-cycloaddition (see later regarding the photolysis). Compared to the corresponding absorption bands of the unsubstituted analogs,[14] those of both the *cis,trans*- and the *trans,trans*-isomers display a significant red shift. This phenomenon is in accordance with the enhanced conjugation, due to the lone pair donating effect of the dimethylamine substituents.

Deviating from the *cis,trans*-isomer of the nitro substituted derivatives (**6**), which could not be dissolved in *n*-hexane at all, the solubility of the *cis,cis*-configuration was suitable enough for both spectral analysis and photolysis. Its absorption spectrum displays two distinct bands; at 306 and 340 nm (Figure 20). These indicate a moderate blue shifts, compared to the corresponding peaks of the unsubstituted analogue.[14] This phenomenon may be attributed to the electron-withdrawing effect of the nitro groups, decreasing the conjugation and, thus, increasing the energy differences between the states involved in the corresponding transition.

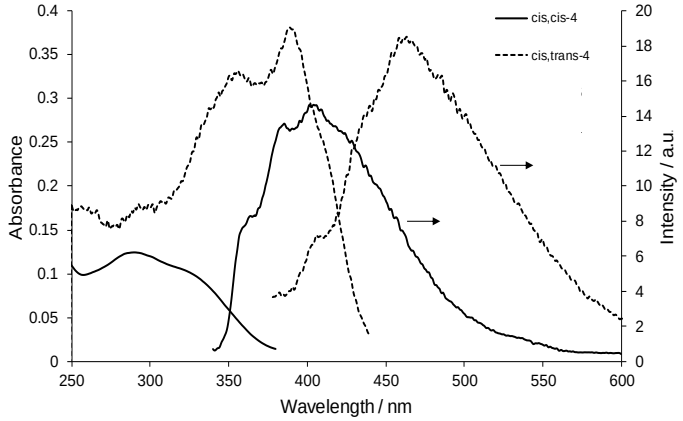

Figure 18. Absorption and emission spectra of the isomers of compound **4** in *n*-hexane. (Due to the low solubility, the absorption spectrum of *cis,trans*-**4** is approached by its excitation spectrum.)

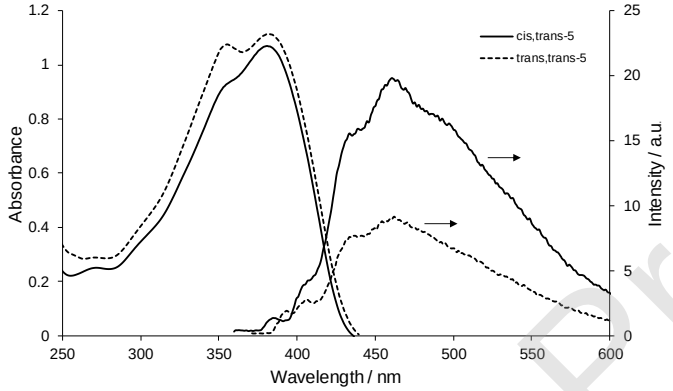

Figure 19. Absorption and emission spectra of the isomers of compound **5** in *n*-hexane.

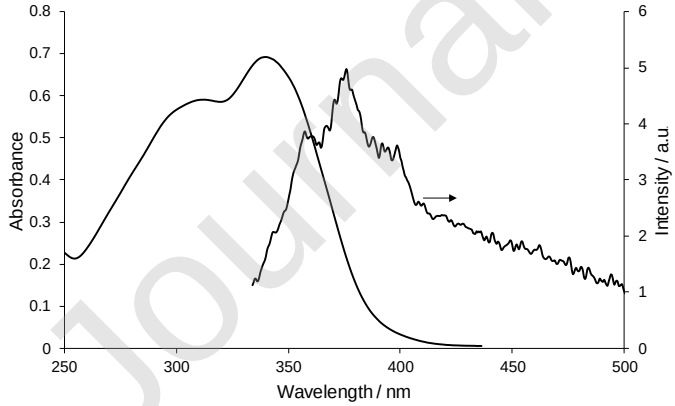

Figure 20. Absorption and emission spectra of *cis,cis*-**6** in *n*-hexane.

Emission spectra of 4-6

Generally, the compounds with double butadiene structure displayed less intense emissions than the one-chain analogues. This phenomenon can be attributed to the higher probability of the relaxation of the excited molecules via vibrational routes.

Interestingly, deviating from the analog with one butadiene chain (*cis*-**1**), the fluoro-substituted derivative (*cis,cis*-**4**) displayed separated bands with 385 and 405 nm wavelength (Figure 18). (The intensity of the latter one was a bit higher.) The emission spectrum of the *cis,trans*-**4** isomer, however, is characterized by a single band at 462 nm, along with a shoulder at 437 nm). These energies clearly indicate, that the *trans* configuration results in red shifts compared to the bands of the corresponding *cis* isomer, probably due to the stronger conjugation. Besides, the structure of the *trans* configuration is more rigid as indicated by its much lower Stokes-shift (2147 cm^{-1} *vs.* 4940 cm^{-1}).

The *cis,trans*-isomer of the dimethylamine-substituted derivative (**5**) showed a strong band at 463 nm, with a less intense one at 437 nm and a shoulder at 490 nm (Figure 19). The fluorescence of the *trans,trans*-isomer was much weaker with a less resolved spectrum having the main band at 463 nm, strongly merged with another one at 435 nm. In accordance with the fluoro derivatives, the *trans* configuration (in the case of 4, the all-*trans* one) resulted in, even if a slight, red shift of the corresponding bands, due to the stronger conjugation and more rigid structure (the Stokes-shifts are 3311 cm^{-1} and 3211 cm^{-1} for the *cis,trans*-and *trans,trans*-isomer, respectively).

The *cis,cis*-**6** isomer, the only nitro derivative soluble in *n*-hexane, displayed a well-resolved emission spectrum with three separate bands at 360, 376 (main), and 394 nm (Figure 20). These bands are slightly blueshifted, compared to those of the corresponding unsubstituted parent compound.[14] This observation is in accordance with that regarding the absorption bands and may be attributed to the electron-withdrawing effect of the nitro groups as discussed there.

Photolysis of diarylbutadienyl derivatives 4-6

The photolysis of the isomers of the **4**, **5**, and **6** compounds which could be dissolved in appropriate concentrations in *n*-hexane (at wavelengths corresponding to their main absorption bands; 313 nm for **4** and 366 nm for **5** and **6**) led to a relatively fast isomerization as the primary photochemical reaction, similarly to the analogous compounds with one butadiene chain.

Accordingly, from the fluoro-substituted compounds, in the case of *cis,cis*-**4**, the spectral change upon irradiation displayed significant red shifts; from 290 to 308 nm and from 327 to 346 nm, indicating isomerisation to *trans* configuration at one of the butadiene chains (Figure 21). Further spectral changes, i.e., absorption decays could not be kinetically measured because of the very low concentration. For *cis,trans*-**4**, which could be dissolved in even lower concentration, the change of the excitation spectrum was followed upon irradiation. This hardly showed shifts of the distinct bands, but their intensity ratios altered, meanwhile also the absolute intensities decreased. These phenomena indicated both isomerization and a transformation into one or more product(s) with less conjugated bond structure. This observation is in accordance with the result of the preparative photolysis, according to which a cycloaddition products (**9** and **10**, with yields of 36 %and 18%, respectively). Notably, even the higher yield is much lower than that regarding the analogous one (**7**) formed from fluoro-substituted derivative with one butadiene chain, indicating a less reactivity of the former compound. This result can be attributed to the more possibilities of dissipation of the excitation energy through various vibration modes.

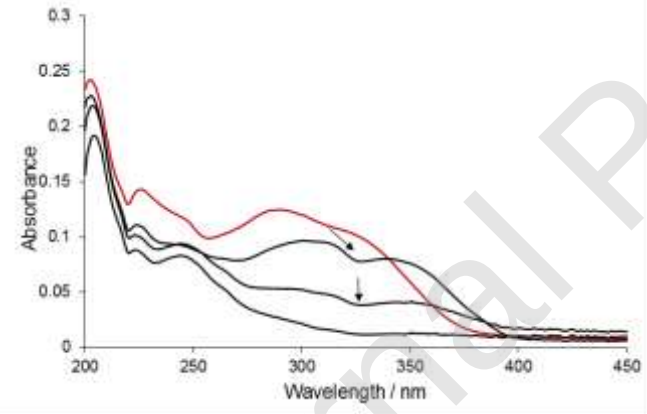

Figure 21. Spectral change during the irradiation of *cis,cis*-**4** in *n*-hexane after 0 (red), 350, 4030, and 8830 s (λ_{ir} = 313 nm, l = 1 cm).

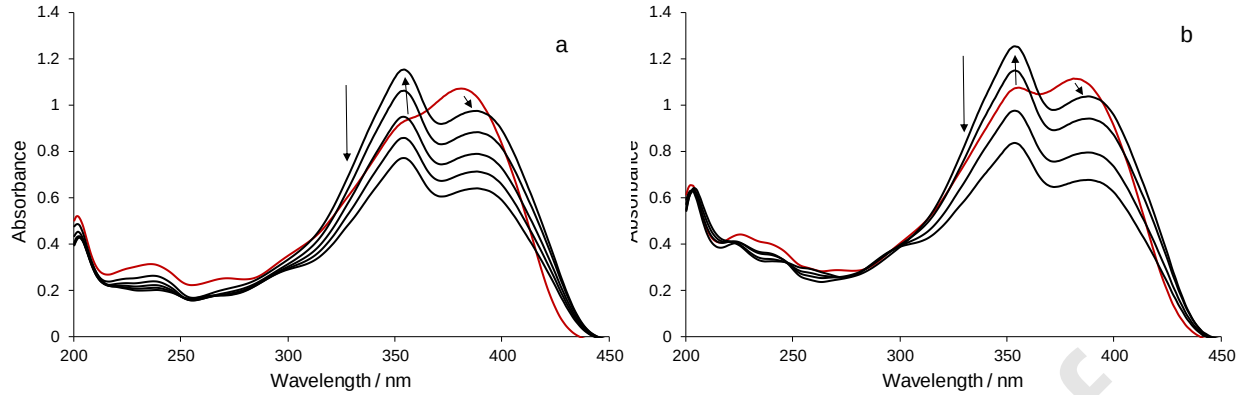

Figure 22. Spectral change during the irradiation of *cis,trans*-**5** (a) after 0 (red), 260, 2040, 4440, 6600, 8760 s; and *trans,trans*-**5** (b) after 0 (red), 280, 2560, 5920, 8800 s (in *n*-hexane, λ_{ir} = 366 nm, l = 1 cm).

Irradiations of the dimethylamine substituted derivatives (*cis,trans*- and *trans,trans*-**5**) resulted in rather fast isomerizations as shown in Figure 22 – the spectral changes in both cases displayed red shifts. Accordingly, the quantum yields are rather high; 0.89 for the *cis,trans*- and 0.74 for the *trans,trans*-configurations, in agreement with the results regarding the corresponding compounds with one butadiene chain. However, the absorption decays following the efficient isomerizations were very slow as it is manifested in the quantum yields (0.0022 and 0.0027 for the *cis,trans*- and the *trans,trans*-isomers, respectively). These values on order of magnitude lower than those in the case of the analogous compounds with one butadiene chain. This is the consequence of the much more efficient relaxation of the excited states *via* vibrational processes very efficiently competing with the transformation reactions. These results are in a good accordance with the observations at the preparative photolyses, where no appreciable amounts of end-products were obtained.

From the nitro-substituted compounds (**6**), only the *cis,cis*-isomer could be dissolved in *n*-hexane. Also its irradiation led to a moderately fast isomerization as indicated by the red shift of the main bands, suggesting a transformation from *cis*- to *trans*-configuration (Figure 23). The quantum yield of this primary photoreaction was 0.125, which is considerably lower than the corresponding values obtained for the other compounds in this study. This could also be the consequence of the more efficient energy dissipation processes.

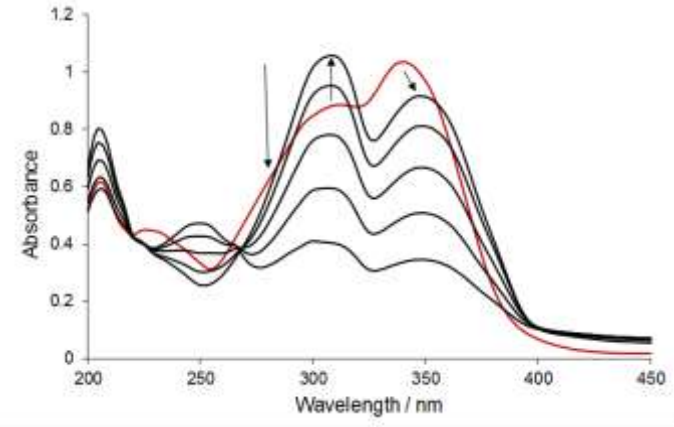

Figure 23. Spectral change during the irradiation of *cis,cis*-**6** in *n*-hexane after 0 (red), 460, 1270, 3640, 5920 and 8800 s (λ_{ir} = 366 nm, l = 1 cm).

The absorption decay and the corresponding quantum yield regarding the transformation of the photo-isomer was very similar to those observed in the case of the analogous one-butadiene-chained derivative. This is also in accordance with the lack of a stabile end-product of the preparative photolysis of *cis,cis*-**6**, confirming the very low reactivity of the nitro-substituted photo-isomers.

Conclusion

Novel *p*-fluoro, *p*-dimethylamino and *p*-nitro substituted arylbutadiene derivatives were synthesized by Wittig reaction and their diverse photochemistry and photophysics were established and explained. Under excitation mono- and difluoro derivatives undergo photoinduced intramolecular cycloaddition giving the *endo*-benzobicyclo[3.2.1]octadiene photoproducts in 87% and 36% yields, respectively. The parent mono-dimethylamino substituted derivative undergoes the same reaction type giving the photocycloadduct in 24% yield and with incomplete consumption, whereas its di-dimethylamino analogue shows only geometrical isomerization due to the steric effect of the substituents. Notably, the primary photochemical step for each compound is a fast cis-trans isomerization, the quantum efficiency of which is close to unity in the case of the derivatives with one-butadiene-chain. Its efficiencies for the double-chain analogues are lower because of the higher probability of vibrational relaxation of their excited-state molecules. The isomers of mono- and dinitro derivatives cannot react further due to the strong electron-withdrawing effect of the NO_2 group, hindering intramolecular cycloaddition. The emissions of all of the compounds studied are rather weak, especially those of the double-chain derivatives, because

the radiative decay cannot efficiently compete with the primary photochemical step and the vibrational relaxation. The computational investigation of energy profiles of Wittig's synthesis of **3**-**6** gave rationalization of stereochemistry of obtained products, showing that for the fluoro- and nitro-derivatives, the stereochemistry of the final product is determined by the second phase of the synthesis when activation energy for the occurrence of the oxaphosphetane-1' (OP1') that results in *E,E* stereoisomer is too high. In dimethylamino-derivative **5**, the stereochemistry is defined in the first stage when *Z*-monoarylbutadiene does not occur due to the too high energy barrier for the formation of the oxaphosphoetane-1 (OP1). Conformational analysis of compounds **1**-**6** showed that the electron-inductive effect of substituents did not make any relevant influence on the energy distribution of conformers, and the most stable conformations of all compounds depend mostly on steric factors.

Experimental section

General remarks: Petroleum ether (PE), bp 40-60 ºC, was used. Solvents were purified by distillation. Column chromatography was carried out on columns with silica gel (Fluka 0.063-0.2 nm and Fluka 60 Å, technical grade). TLC was carried out using plates coated with silica gel (0.2 mm, 0.5 mm, 1.0 mm, Kiselgel 60 F_{254}). Organic layers were routinely dried with anhydrous $MgSO_4$ and evaporated using a rotary evaporator. ^1H and ^{13}C NMR spectra were recorded on a spectrometer at 600 MHz. All NMR spectra were measured in $CDCl_3$ using tetramethylsilane as reference. The assignments of the signals are based on 2D-CH correlations and 2D-HH-COSY correlations. The following abbreviations were used: s - singlet; d - doublet; t - triplet; q - quartet, dd - doublet of doublets; m - multiplet and br - broad, PE – petroleum ether, E - ether. For quantum yield measurements a photolysis equipment, containing a 400 W XeHg lamp (Oriel) and a monochromator (AMKO) was used. Irradiation wavelengths were 313 and 366 nm. Incident light intensity was determined with a thermopile calibrated by ferrioxalate actinometry. Typically, the irradiations were carried out with 3.0-cm^3 solutions in 1-cm cells at room temperature. HPLC grade *n*-hexane anf EtOH were used as solvents in these experiments. During the photolyses, the reaction mixtures were continuously homogenized by magnetic stirring. Following the change of the absorption spectrum of the solution photolyzed, the quantum yield for the photochemical transformation of the starting material was determined from the initial rate calculated from the absorbance versus time plot at a characteristic wavelength. Absorption spectra were recorded by

using a diode array spectrophotometer (Specord S600). For the measurement of fluorescence spectra, a high-sensitivity spectrofluorimeter (Horiba) was applied. This equipment supplemented with a time-correlated single-photon counting accessory was applied for determination of fluorescence lifetimes, too. Quinine bisulphate (in $0.5MH_2SO_4$) was utilized as reference for determination of the fluorescence quantum yields. Each compound studied was excited at the wavelength of its absorption maximum. Luminescence spectra were corrected for detector sensitivity. Mass spectra were obtained on a UPLC-MS system. Melting points were obtained using a microscope equipped apparatus and are uncorrected. HRMS analysis were carried out on a mass spectrometer (MALDI TOF/TOF analyzer), equipped with Nd:YAG laser operating at 355 nm with firing rate 200 Hz in the positive (H+) or negative (-H) ion reflector mode. Irradiation experiments of compound solutions were performed in a tightly closed vessel in a photochemical reactor (Rayonet and Luzchem) equipped with the UV lamps (313 and 366 nm). The solvents were removed on the rotary evaporator under reduced pressure in a ventilated hood.

General procedure for synthesis of starting substrates 1-3 used in photochemical reactions:[22] To a stirred solution of the diphosphonium salt of α,α'-*o*-xylenedibromide (5.5 mmol) in absolute ethanol (100 mL, 3 Å sieves), corresponding aldehydes (1.1 eq) were added. A solution of sodium ethoxide (1.1 eq in 15 mL of absolute ethanol) was added dropwise and reaction mixture stirred under nitrogen for 1h at RT. Under a stream of dry nitrogen, gaseous formaldehyde (obtained by decomposition of paraformaldehyde used in excess, (1.0 g) was introduced together with sodium ethoxide solution, which was added dropwise. The reaction mixture was stirred overnight at RT. After removal of the solvent, the residue was worked up with ice-water and extracted with toluene (5 x 30 ml). The toluene extracts were dried with anhydrous $MgSO_4$. Evaporation of solvent under reduced pressure afforded crude mixture of geometrical isomers. The crude reaction mixture was purified and the isomers of **1-3** were separated by repeated column chromatography on silica gel. The first fractions yielded *cis*- and the last fractions *trans*-isomers depending on the starting aldehydes. Characterization data of the synthesized compounds **1-3** are given below.

1-((1*Z*,3*E*)-4-(4-fluorophenyl)buta-1,3-dien-1-yl)-2-vinylbenzene (*cis*-1) and 1-((1*E*,3*E*)-4-(4-fluorophenyl)buta-1,3-dien-1-yl)-2-vinyl-benzene (*trans*-1)[22] Column chromatography on silica gel using petroleum ether as eluent afforded 300 mg (70%) of mixture of isomers of compound **1**. According to ^{1}H NMR spectrum the ratio of isomers was 48% of *cis*-**1** and 52% of *trans*-**1**.

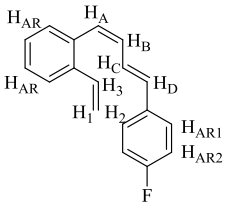

cis-**1**

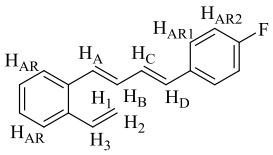

trans-**1**

cis-**1**: yellow oil; R_f = 0.60 (petroleum ether); ^{1}H NMR ($CDCl_3$, 600 MHz) δ/ppm: 7.60 (d, 1H, J = 7.6 Hz, H_{AR2}), 7.33 (m, 5H, H_{AR2}, H_{AR1}, H_{AR}), 6.99 (t, 2H, J = 11.2 Hz, H_{AR}), 6.97-6.90 (m, 2H, H_3, H_C), 6.67 (d, 1H, J = 11.7 Hz, H_A), 6.65 (d, 1H, J = 15.4 Hz, H_D), 6.50 (t, 1H, J = 11.7 Hz, H_B), 5.73 (d, 1H, J = 17.1 Hz, H_1), 5.33 (d, 1H, J = 11.0 Hz, H_2); ^{13}C NMR ($CDCl_3$, 150 MHz) δ/ppm: 136.3 (s), 135.7 (s), 135.4 (s), 135.2 (s), 134.8 (d), 133.1 (d), 131.6 (d), 130.9 (d), 130.6 (d), 130.2 (d), 129.6 (d), 127.9 (2d), 127.8 (2d), 125.7 (d), 124.4 (d), 115.4 (t); MS *m/z* (%, fragment) (EI): 250 (100, M^+); HRMS (*m/z*) for $C_{18}H_{15}F$: $[M+H]^+_{calcd}$ = 251.1157, $[M+H]^+_{found}$ = 251.1169.

trans-**1**: yellow oil; R_f = 0.59 (petroleum ether); ^{1}H NMR ($CDCl_3$, 600 MHz) δ/ppm: 7.52 (d, 1H, J = 7.5 Hz, H_{AR2}), 7.45 (d, 1H, J = 7.5 Hz, H_{AR2}), 7.42-7.38 (m, 2H, H_{AR1}), 7.28-7.22 (m, 2H, H_{AR}), 7.07 (t, 1H, J = 11.1 Hz, H_{AR}), 7.02 (t, 2H, J = 8.4 Hz, H_{AR}, H_3), 6.96 (d, 1H, J = 15.2 Hz, H_A/H_D), 6.89 (dd, 1H, J = 15.3; 10.4 Hz, H_B/H_C), 6.82 (dd, 1H, J = 15.3 Hz; 10.4 Hz, H_B/H_C), 6.63 (d, 1H, J = 15.6 Hz, H_A/H_D), 5.63 (dd, 1H, J = 17.4; 1.3 Hz, H_1), 5.37 (dd, 1H, J = 11.4; 1.3 Hz, H_2); ^{13}C NMR ($CDCl_3$, 150 MHz) δ/ppm: 140.7 (s), 135.5 (s), 134.8 (s), 134.6 (s), 134.4 (d), 131.2 (d), 130.8 (d), 130.6 (d), 129.8 (d), 128.7 (2d), 127.3 (2d), 127.1 (d), 126.2 (d), 125.3 (d), 116.1 (t); MS *m/z* (%, fragment) (EI): 250 (100, M^+); HRMS (*m/z*) for $C_{18}H_{15}F$: $[M+H]^+_{calcd}$ = 251.1157, $[M+H]^+_{found}$ = 251.1171.

***N*,*N*-dimethyl-4-((1*E*,3*Z*)-4-(2-vinylphenyl)buta-1,3-dien-1-yl)aniline (*cis*-2) and *N*,*N*-dimethyl-4-((1*E*,3*E*)-4-(2-vinylphenyl)buta-1,3-dien-1-yl)aniline (*trans*-2)[22]** Column chromatography on silica gel using petroleum ether/dichloromethane (3:1) as eluent afforded 250 mg (78%) of mixture of isomers of compound **1**. According to ^{1}H NMR spectrum the ratio of isomers was 51% *cis*-**2** and 49% of *trans*-**2**.

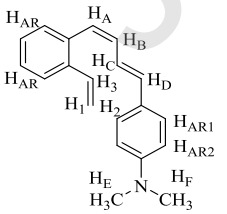

cis-**2**

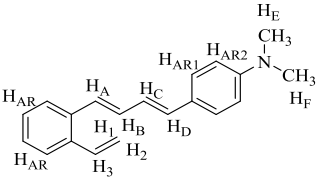

trans-**2**

cis-**2**: yellow oil; R_f = 0.60 (petroleum ether/dichloromethane = 3:1); ^{1}H NMR (CDCl3, 600 MHz) δ/ppm: 7.55-7.50 (m, 1H, H_{AR2}), 7.34-7.29 (m, 1H, H_{AR2}), 7.27-7.19 (m, 4H, H_{AR1}, H_{AR}), 6.96-6.78 (m, 2H, H_{AR}), 6.62 (d, 2H, J = 10.9 Hz, H_3, $H_{A/D}$), 6.58 (d, 1H, J = 11.4 Hz, H_A/H_D), 6.44 (t, 2H, J = 11.4 Hz, H_B, H_C), 5.65 (dd, 1H, J = 17.4; 1.2 Hz, H_1), 5.25 (dd, 1H, J = 11.1; 1.2 Hz, H_2), 2.92 (s, 6H, H_E, H_F); ^{13}C NMR ($CDCl_3$, 150 MHz) δ/ppm: 148.9 (s), 135.9 (s), 135.7 (s), 134.8 (d), 134.3 (d), 131.3 (d), 129.7 (d), 127.2 (2d), 126.6 (d), 126.1 (d), 125.1 (d), 114.7 (t), 111.8 (2d), 39.8 (q); MS *m/z* (%, fragment) (EI): 275 (100, M^+); HRMS (*m/z*) for $C_{18}H_{21}F$: $[M+H]^+_{calcd}$ = 276.1673, $[M+H]^+_{found}$ = 276.1666.

trans-**2**: yellow oil; R_f = 0.60 (petroleum ether/dichloromethane = 3:1); ^{1}H NMR ($CDCl_3$, 600 MHz) δ/ppm: 7.54 (d, 1H, J = 7.8 Hz, H_{AR2}), 7.47 (d, 1H, J = 7.1 Hz, H_{AR2}), 7.31 (d, 2H, J = 9.0 Hz, H_{AR1}), 7.27 (dt, 1H, J = 7.7; 1.2 Hz, H_{AR}), 7.19 (dt, 1H, J = 7.7; 1.2 Hz, H_{AR}), 7.11 (dd, 1H, J = 17.2; 11.2 Hz, H_{AR}), 6.91-6.81 (m, 3H, H_{AR}, H_3, H_B /H_C), 6.71 (d, 2H, J = 9.0 Hz, H_A, H_D), 6.64 (d, 1H, J = 14.8 Hz, H_A/H_D), 5.65 (dd, 1H, J = 17.6; 1.5 Hz, H_1), 5.37 (d, 1H, J = 10.9; 1.5 Hz, H_2), 2.99 (s, 6H, H_E, H_F); ^{13}C NMR ($CDCl_3$, 150 MHz) δ/ppm: 150.1 (s), 136.0 (s), 135.9 (s), 135.2 (d), 133.5 (d), 132.2 (d), 127.8 (s), 127.6 (2d), 127.1 (d), 126.6 (d), 125.8 (s), 125.7 (d), 125.4 (d), 116.2 (t), 112.4 (2d), 40.4 (2q); MS *m/z* (%, fragment) (EI): 275 (100, M^+); HRMS (*m/z*) for $C_{18}H_{21}F$: $[M+H]^+_{calcd}$ = 276.1673, $[M+H]^+_{found}$ = 276.1684.

1-((1*Z*,3*E*)-4-(4-nitrophenyl)buta-1,3-dien-1-yl)-2-vinylbenzene (*cis*-3) and 1-((1*E*,3*E*)-4-(4-nitrophenyl)buta-1,3-dien-1-yl)-2-vinylbenzene (*trans*-3)[22] Column chromatography on silica gel using petroleum ether/dichloromethane (50%) as eluent afforded 200 mg (56%) of mixture of isomers of compound **3**. According to ^{1}H NMR spectrum the ratio of isomers was 31% of *cis*-**3** and 69% of *trans*-**3**.

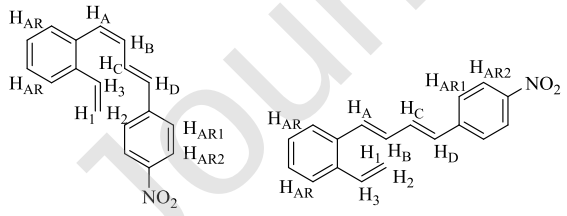

cis-**3** *trans*-**3**

cis-**3**: yellow crystals; mp = 96–98 °C; R_f = 0.68 (petroleum ether/dichlormethane = 1:1); ^{1}H NMR ($CDCl_3$, 600 MHz); δ/ppm 8.13 (d, 2H, J = 8.7 Hz, H_{AR2}), 7.58 (d, 1H, J = 7.5 Hz, H_{AR}), 7.44 (d, 2H, J = 8.7 Hz, H_{AR1}), 7.36-7.26 (m, 3H, H_{AR}), 7.15 (dd, 1H, J = 15.7; 11.3 Hz, H_C), 6.88 (dd, 1H, J = 17.3; 10.9 Hz, H_3), 6.80 (d, 1H, J = 11.3 Hz, H_A), 6.711 (d, 1H, J = 15.7 Hz, H_D), 6.52 (t, 1H,

J = 11.3 Hz, H_B), 5.70 (d, 1H, J = 17.3; 1.2 Hz, H_1), 5.31 (d, 1H, J = 10.9; 1.2 Hz, H_2); ^{13}C NMR ($CDCl_3$, 150 MHz) δ/ppm: 136.4 (s), 135.7 (2s), 135.4 (s), 135.1 (d), 133.0 (d), 130.7 (d), 130.3 (d), 129.4 (d), 128.8 (2d), 127.4 (2d), 127.0 (d), 126.1 (d), 125.9 (d), 125.4 (d), 115.7 (t); MS *m/z* (%, fragment) (EI): 270 (100, M^+); HRMS (*m/z*) for $C_{18}H_{15}NO_2$: $[M+H]^+_{calcd}$ = 271.1102, $[M+H]^+_{found}$ = 271.1087.

trans-**3**: yellow-orange powder; mp = 127–129 °C; R_f = 0.68 (petroleum ether/dichlormethane = 1:1); ^{1}H NMR ($CDCl_3$, 600 MHz) δ/ ppm: 8.19 (d, 2H, J = 8.6 Hz, H_{AR2}), 7.55 (d, 2H, J = 8.6 Hz, H_{AR1}), 7.55-7.52 (m, 1H, H_{AR}), 7.49-7.44 (m, 1H, H_{AR}), 7.31-7.26 (m, 2H, H_{AR}), 7.13 (dd, 1H, J = 17.6; 11.3 Hz, H_3), 7.11 (d, 1H, J = 16.4 Hz, H_A/H_D), 7.05 (dd, 1H, J = 16.4; 10.5 Hz, H_B), 6.86 (dd, 1H, J = 15.8; 10.5 Hz, H_C), 6.69 (d, 1H, J = 15.6 Hz, H_A/H_D), 5.63 (d, 1H, J = 17.6 Hz, H_1), 5.38 (d, 1H, J = 11.3 Hz, H_2); ^{13}C NMR ($CDCl_3$, 150 MHz) δ/ppm: 135.8 (s), 135.4 (s), 134.7 (s), 134.3 (d), 132.6 (s), 131.0 (d), 130.4 (d), 130.2 (d), 129.6 (d), 128.4 (2d), 127.3 (d), 127.2 (d), 126.9 (2d), 126.4 (d), 125.4 (d), 116.1 (t); MS *m/z* (%, fragment) (EI): 270 (100, M^+); HRMS (*m/z*) for $C_{18}H_{15}NO_2$: $[M+H]^+_{calcd}$ = 271.1102, $[M+H]^+_{found}$ = 271.1117.

General procedure for synthesis of starting substrates 4-6 used in photochemical reactions: To a stirred solution of the diphosphonium salt of α,α'-*o*-xylenedibromide (5.5 mmol) in absolute ethanol (100 mL, 3 Å sieves), corresponding aldehydes (2.1 eq) were added. A solution of sodium ethoxide (2.1 eq in 30 mL of absolute ethanol) was added dropwise and reaction mixture stirred under nitrogen for 1h at RT. The reaction mixture was stirred overnight at RT. After removal of the solvent, the residue was worked up with ice-water and extracted with toluene (5 x 30 ml). The toluene extracts were dried with anhydrous $MgSO_4$. Evaporation of solvent under reduced pressure afforded crude mixture of geometrical isomers. The crude reaction mixture was purified and the isomers of **4-6** were separated by repeated column chromatography on silica gel using petroleum ether/diethyl ether (0-5%) as eluent. The first fractions yielded *cis*- or *cis,cis*- and the last fractions *trans*- or *trans,trans*-isomers depending on the starting aldehydes. Characterization data of the synthesized compounds **4-6** are given below.

1,2-bis((1*Z*,3*E*)-4-(4-fluorophenyl)buta-1,3-dien-1-yl)benzene (*cis,cis*-4) and 1-((1*E*,3*E*)-4-(4-fluorophenyl)buta-1,3-dien-1-yl)-2-((1*Z*,3*E*)-4-(4-fluorophenyl)buta-1,3-dien-1-yl)benzene (*cis,trans*-4): Column chromatography on silica gel using petroleum ether/diethyl ether (0-5%) as eluent afforded 163 mg (49%) of mixture of isomers of compound **4**. According to ^{1}H NMR ratio of isomers was 40% of *cis,cis*-**4** and 60% of *cis,trans*-**4**. Additionally, column chromatography on

silica gel using petroleum ether/diethyl ether (0-5%) as eluent afforded 10 mg of pure *cis,cis*-**4** and 110 mg of pure *cis,trans*-**4** isomer.

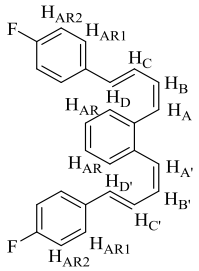

cis,cis-**4**

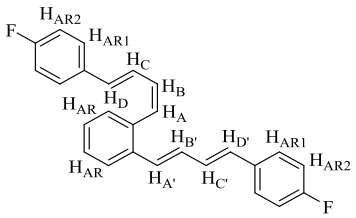

cis,trans-**4**

cis,cis-**4**: colourless oil; R_f = 0.65 (petroleum ether/ diethyl ether = 9:1); ^{1}H NMR ($CDCl_3$, 600 MHz) δ/ppm: 7.44-7.38 (m, 2H, H_{AR}), 7.35-7.27 (m, 8H, $H_{AR1, AR2}$), 6.97-7.07 (m, 2H, H_{AR}), 6.91 (t, 2H, J = 11.1 Hz, H_B/H_C), 6.62 (d, 2H, J = 15.6 Hz, H_A/H_D), 6.53 (d, 2H, J = 11.1 Hz, H_A/H_D), 6.42 (dd, 2H, J = 15.6 Hz; 11.1 Hz, H_B/H_C); ^{13}C NMR ($CDCl_3$, 150 MHz) δ/ppm: 164.1 (s), 160.6 (s), 136.5 (s), 133.3 (d), 130.7 (2d), 130.1 (d), 129.6 (2d), 128.0 (d), 127.1 (d), 125.4 (d), 125.3 (d); MS *m/z* (%, fragment) (EI): 370 (100, M^+); HRMS (*m/z*) for $C_{26}H_{20}F_2$: $[M+H]^+_{calcd}$ = 371.1533, $[M+H]^+_{found}$ = 371.1552.

cis,trans-**4**: yellow crystals; mp = 257-260 °C; R_f = 0.65 (petroleum ether/ diethyl ether = 9:1); ^{1}H NMR ($CDCl_3$, 600 MHz), δ/ppm: 7.61 (d, 1H, J = 8.3 Hz, H_{AR}), 7.40-7.34 (m, 3H, H_{AR}), 7.29 (m, 4H, H_{AR1}), 7.04-6.90 (m, 5H, $4H_{AR2}$, $H_{B(')}/H_{C(')}/H_B/H_C$), 6.87 (m, 3H, $H_A/H_D/H_{B(')}/H_{C(')}$), 6.69-6.59 (m, 3H, $H_{A(')}/H_{D(')}$), 6.50 (dd, 1H, J = 11.2; 10.6 Hz, H_B/H_C); ^{13}C NMR ($CDCl_3$, 150 MHz) δ/ppm: 162.7 (s), 162.6 (s), 155.5 (s), 135.4 (s), 135.3 (s), 133.0 (s), 132.7 (d), 131.2 (d), 130.6 (2d), 130.3 (d), 130.2 (d), 129.9 (2d), 128.9 (d), 128.8 (2d), 127.6 (d), 127.4 (d), 127.1 (2d), 126.7 (d), 125.0 (d), 124.7 (d), 115.2 (d), 115.0 (d); MS *m/z* (%, fragment) (EI): 370 (100, M^+); HRMS (*m/z*) for $C_{26}H_{20}F_2$: $[M+H]^+_{calcd}$ = 371.1533, $[M+H]^+_{found}$ = 371.1549.

1,2-bis((1*E*,3*E*)-4-(4-dimethylaminophenyl)buta-1,3-dien-1-yl)benzene (*trans,trans*-5) and 1-((1*E*,3*E*)-4-(4-dimethylamino-phenyl)buta-1,3-dien-1-yl)-2-((1*Z*,3*E*)-4-(4-dimethylaminophenyl)-buta-1,3-dien-1-yl)benzene (*cis,trans*-5): Column chromatography on silica gel using petroleum ether/diethyl ether (0-5%) as eluent afforded 210 mg (64%) of mixture of isomers of compound **5**. According to ^{1}H NMR ratio of isomers was 45% of *cis,trans*-**5** and 55% of *trans,trans*-**5**. Additionally, column chromatography on silica gel using petroleum ether/diethyl ether (0-5%) as eluent afforded 75 mg of pure *cis,trans*-**5** and 12 mg of pure *trans,trans*-**5**.

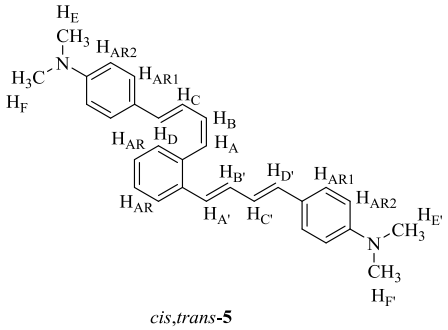

cis,trans-**5**

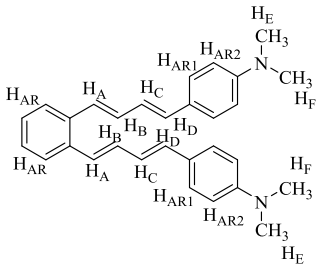

trans,trans-**5**

cis,trans-**5**: orange powder; mp = 237-239 °C; R_f = 0.69 (petroleum ether/ diethyl ether = 9:1); ^{1}H NMR ($CDCl_3$, 600 MHz) δ/ppm: 7.59 (d, 1H, J = 8.3 Hz, H_{AR}), 7.33 (d, 1H, J = 8.3 Hz, H_{AR}), 7.32 (d, 2H, J = 8.8 Hz, H_{AR1}), 7.27-7.22 (m, 1H, H_{AR}), 7.24 (d, 2H, J = 8.8 Hz, H_{AR1}), 7.21 (t, 1H, J = 8.3 Hz, H_{AR}), 6.93 (d, 1H, J = 15.5 Hz, $H_{A(')}/H_{D(')}$), 6.90 (t, 1H, J = 11.1 Hz, H_B/H_C), 6.88 (d, 1H, J = 10.9 Hz, H_A/H_D), 6.81 (dd, 1H, J = 15.5; 10.9 Hz, H_B/H_C), 6.78 (dd, 1H, J = 15.5; 10.5 Hz, H_B/H_C), 6.67 (d, 2H, J = 8.8 Hz, H_{AR2}), 6.63 (d, 2H, J = 8.8 Hz, H_{AR2}), 6.60 (d, 1H, J = 15.5 Hz, $H_{A(')}/H_{D(')}$), 6.53-6.46 (m, 2H, $H_{B(')}/H_{C(')}$, $H_{A(')}/H_{D(')}$), 2.97 (s, 6H, H_E/H_F), 2.93 (s, 6H, $H_{E(')}/H_{F(')}$); ^{13}C NMR ($CDCl_3$, 150 MHz) δ/ppm: 160.5 (s), 157.5 (s), 154.6 (s), 150.1 (s), 105.0 (s), 136.3 (s), 135.9 (d), 134.7 (d), 133.3 (d), 131.6 (d), 131.5 (d), 130.5 (d), 128.3 (d), 127.7 (2d), 127.5 (2d), 127.1 (d), 126.9 (d), 126.5 (d), 125.8 (d), 125.7 (d), 125.2 (d), 121.5 (d), 113.7 (2d), 113.4 (2d), 40.4 (q), 40.3 (q); MS *m/z* (%, fragment) (EI): 420 (100, M^+); HRMS (*m/z*) for $C_{30}H_{32}N_2$: $[M+H]^+_{calcd}$ = 421.2565, $[M+H]^+_{found}$ = 421.2584.

trans,trans-**5**: orange powder; mp = 249-251 °C; R_f = 0.67 (petroleum ether/ diethyl ether = 9:1); ^{1}H NMR ($CDCl_3$, 600 MHz) δ/ppm: 7.59 (d, 2H, J = 9.1 Hz, H_{AR}), 7.50 (d, 2H, J = 8.5 Hz, H_{AR}), 7.35 (d, 4H, J = 8.5 Hz, H_{AR1}), 7.26-7.16 (m, 2H, H_B/H_C), 6.92-6.81 (m, 2H, H_B/H_C), 6.68 (d, 4H, J = 8.5 Hz, H_{AR2}), 6.66 (d, 2H, J = 15.5 Hz, H_A/H_D), 6.63 (d, 2H, J = 15.5 Hz, H_A/H_D), 2.96 (s, 12H, H_E, H_F); ^{13}C NMR ($CDCl_3$, 150 MHz) δ/ppm: wasn't successfully recorded due to the fast isomerization and small amount of desired isomer isolated; MS *m/z* (%, fragment) (EI): 420 (100, M^+); HRMS (*m/z*) for $C_{30}H_{32}N_2$: $[M+H]^+_{calcd}$ = 421.2565, $[M+H]^+_{found}$ = 421.2578.

1,2-bis((1*Z*,3*E*)-4-(4-nitrophenyl)buta-1,3-dien-1-yl)benzene (*cis,cis*-6) and 1-((1*E*,3*E*)-4-(4-nitrophenyl)buta-1,3-dien-1-yl)-2-((1*Z*,3*E*)-4-(4-nitrophenyl)buta-1,3-dien-1-yl)benzene (*cis,trans*-6): Column chromatography on silica gel using petroleum ether/diethyl ether (0-5%) as eluent afforded 127 mg (45%) of mixture of isomers of compound **6**. According to ^{1}H NMR ratio of isomers was 50% of *cis,cis*-**6** and 50% of *cis,trans*-**6**. Additionally, column chromatography on

silica gel using petroleum ether/diethyl ether (0-5%) as eluent afforded 22 mg of pure *cis,cis*-**6** and 17 mg of pure *cis,trans*-**6**.

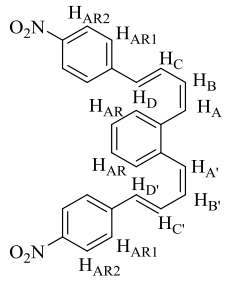

cis,cis-**6**

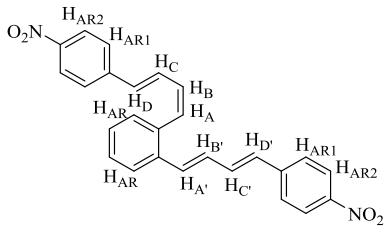

cis,trans-**6**

cis,cis-**6**: yellow powder; mp = 214-216 °C; R_f = 0.60 (petroleum ether/dichloromethane = 9:1); ^{1}H NMR ($CDCl_3$, 600 MHz) δ/ppm: 8.16 (d, 2H, J = 9.1 Hz, H_{AR}), 8.10 (d, 4H, J = 8.5 Hz, H_{AR1}), 7.52 (d, 2H, J = 8.7 Hz, H_{AR}), 7.45 (d, 4H, J = 8.5 Hz, H_{AR2}), 7.42 (d, 2H, J = 15.6 Hz, H_D), 7.26-7.20 (m, 2H, H_B/H_C) 6.70 (d, 2H, J = 11.6 Hz, H_A), 6.49 (t, 2H, J = 11.1 Hz, H_B/H_C); ^{13}C NMR ($CDCl_3$, 150 MHz) δ/ppm: 143.6 (s), 132.4 (d), 132.2 (d), 130.3 (d), 130.2 (d), 130.1 (s), 129.8 (d), 127.7 (2d), 126.8 (d), 124.2 (s), 124.1 (2d); MS *m/z* (%, fragment) (EI): 424 (100, M^+); HRMS (*m/z*) for $C_{26}H_{20}N_2O_4$: $[M+H]^+_{calcd}$ = 424.1423, $[M+H]^+_{found}$ = 424.1441.

cis,trans-**6**: yellow powder; mp = 220-222 °C; R_f = 0.60 (petroleum ether/dichloromethane = 9:1); ^{1}H NMR ($CDCl_3$, 600 MHz) δ/ppm: 8.15 (d, 2H, J = 8.5 Hz, H_{AR2}), 8.10 (d, 2H, J = 8.5 Hz, H_{AR2}), 7.67 (d, 1H, J = 7.6 Hz, H_{AR}), 7.52 (d, 2H, J = 8.3 Hz, H_{AR1}), 7.44 (d, 2H, J = 8.3 Hz, H_{AR1}), 7.39-7.29 (m, 2H, H_{AR}), 7.21-7.09 (m, 1H, H_{AR}), 6.95 (d, 2H, J = 9.5 Hz, H_A/H_D), 6.86-6.65 (m, 4H, $H_{B(')}$/$H_{C(')}$, $H_{A(')}$/$H_{D(')}$), 6.58 (t, 2H, J = 11.2 Hz, H_B/H_C); ^{13}C NMR ($CDCl_3$, 150 MHz) δ/ppm: 163.5 (s), 160.5 (s), 159.5 (s), 151.2 (s), 146.5 (s), 135.5 (s), 133.3 (d), 133.2 (d), 131.7 (d), 131.6 (d), 130.3 (d), 130.1 (d), 130.0 (d), 129.6 (d), 129.2 (d), 127.8 (d), 127.5 (2d), 126.4 (2d), 126.2 (2d), 125.4 (d), 123.6 (d), 123.5 (2d); MS *m/z* (%, fragment) (EI): 424 (100, M^+); HRMS (*m/z*) for $C_{26}H_{20}N_2O_4$: $[M+H]^+_{calcd}$ = 424.1423, $[M+H]^+_{found}$ = 424.1410.

General procedure for synthesis of photoproducts with benzobicyclo[3.2.1]octadiene structures 7-10 by batch photoreaction: A mixture of isomers of the corresponding starting compounds **1-6** (50 mg) were dissolved in toluene (50 mL) and transferred to a quartz or pyrex vessel, purged with argon for 20 minutes, and irradiated with 16 UV lamps at 300 or 350 nm for 5 or 16 h. After removal of the solvent, GC-MS and NMR measurements showed the photoproducts **7-10** depending on the starting derivative. The crude products was purified by column chromatography using petroleum ether/diethylether (0-50%) as eluent. The desired structures of

the photoproducts were obtained in the case of starting mono-*p*-fluorophenyl-butadiene **1** (87% isolated yield of *endo*-**7**) and di-*p*-fluorophenyl-dibutadiene **4** (36% isolated yield of *exo,endo,trans*-**9**) both with complete consumption of starting material, respectively, and in 24% of isolated yield for *endo*-**8** in the case of starting substrate mono-*p*-dimethylamino derivative **2**, with 60% of consumption. Starting compound **4** gave also one minor polycyclic photoproduct *endo,trans*-**10** in 18% of isolated yield in the last fractions of the chromatography column. Nitro derivatives **3** and **6** show photochemical unreactivity and no formation of any cycloadduct. In all cases high-molecular-weight products remained on the column.

(5*R*,6*S*,9*S*)-6-(4-fluorophenyl)-6,9-dihydro-5*H*-5,9-methanobenzo[7]annulene (*endo*-7),[22] ***N*,*N*-dimethyl-4-{tricyclo-[6.3.1.0^{2},^{7}]dodeca-2,4,6,10-tetraen-9-yl}aniline** (*endo*-**8**), **(5*R*,6*S*,9*R*)-6-(4-fluorophenyl)-10-((*E*)-4-fluorostyryl)-6,9-dihydro-5*H*-5,9-methanobenzo[7]annulene (*exo,endo,trans*-9) and (2*S*)-2-(4-fluorophenyl)-8-((*E*)-4-fluorostyryl)-1a,2,3,7b-tetrahydro-1*H*-1,3-methanocyclopropa[a]naphthalene** (*endo,trans*-**10**)

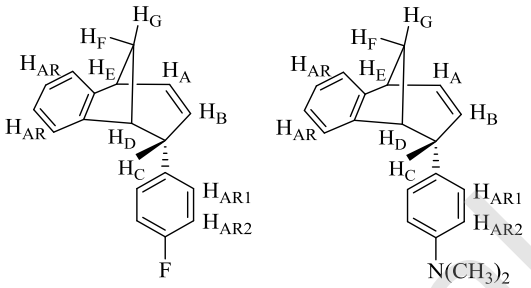

endo-**7** *endo*-**8**

endo-**7**: colourless oil; R_f = 0.60 (petroleum ether); ^{1}H NMR ($CDCl_3$, 600 MHz) δ/ppm: 7.15 (m, 3H, $H_{AR2,}$ H_{AR1}), 7.05 (m, 2H, $H_{AR1,}$ H_{AR}), 6.91-6.80 (m, 1H, H_{AR}), 6.68 (td, 1H, J = 5.2; 2.5 Hz, H_{AR}), 6.42-6.33 (m, 1H, H_A), 6.21 (d, 1H, J = 7.3 Hz, H_{AR}), 5.28 (dt, 1H, J = 7.3; 1.7 Hz, H_B), 4.00-3.93 (m, 1H, H_C), 3.49 (dd, 1H, J = 15.4; 7.4 Hz, H_D), 3.33 (dt, 1H, J = 9.8; 4.7 Hz, H_E), 2.58-2.46 (m, 1H, H_F), 2.38 (d, 1H, J = 9.8 Hz, H_G); ^{13}C NMR ($CDCl_3$, 150 MHz) δ/ppm: 141.8 (s), 138.2 (s), 135.8 (s), 135.5 (s), 135.0 (d), 129.7 (2d), 129.6 (d), 126.2 (2d), 126.1 (d), 125.1 (d), 120.2 (d), 48.6 (d), 45.5 (d), 44.1 (t), 40.3 (d); ^{13}C NMR ($CDCl_3$, 150 MHz) δ/ppm: 141.8 (s), 138.2 (s), 135.8 (s), 135.5 (s), 135.0 (d), 129.7 (2d), 129.6 (d), 126.2 (2d), 126.1 (d), 125.1 (d), 120.2 (d), 48.6 (d), 45.5 (d), 44.1 (t), 40.3 (d); MS *m/z* (%, fragment): 250 (100, M^+), 135 (25); HRMS (*m/z*) for $C_{18}H_{15}F$: $[M+H]^+_{calcd}$ = 251.1157, $[M+H]^+_{found}$ = 251.1172.

endo-**8**: dark yellow oil; R_f = 0.57 (petroleum ether/dichloromethane (30%)); ^{1}H NMR ($CDCl_3$, 600 MHz) δ/ppm: 7.20-7.18 (m, 3H), 7.10 (d, 1H, *J* = 7.2 Hz), 7.05 (t, 1H, *J* = 7.2 Hz), 6.83-6.76 (m, 2H), 6.35 (dt, 1H, *J* = 9.0; 2.5 Hz), 6.20 (d, 1H, *J* = 7.3 Hz), 5.30 (m, 1H), 3.89 (ddd, 1H, *J* = 9.8; 4.7; 2.5 Hz), 3.30 (t, 1H, *J* = 4.7 Hz), 3.21 (dd., 1H, *J* = 6.8; 4.7 Hz), 2.86 (s, 6H), 2.44 (dt, 1H, *J* = 9.9; 4.7 Hz), 2.30 (d, 1H, *J* = 9.9 Hz); ^{13}C NMR ($CDCl_3$, 150 MHz) δ/ppm: 152.6 (s), 152.4 (s), 142.1 (s), 138.3 (s), 135.4 (d), 127.9 (2d), 127.8 (2d), 126.8 (d), 125.5 (d), 125.2 (d), 124.8 (d), 121.7 (d), 53.9 (d), 49.2 (d), 46.9 (d), 46.5 (t), 45.7 (2q); MS *m/z* (%, fragment): 275 (100, M^+), 121 (50); HRMS (*m/z*) for $C_{18}H_{21}N$: $[M+H]^+_{calcd}$ = 275.1722, $[M+H]^+_{found}$ = 275.1733.

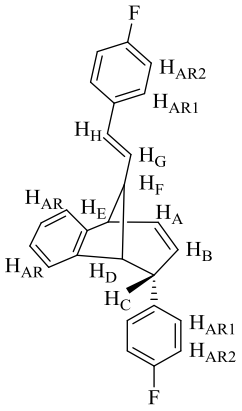

exo,endo,trans-**9**

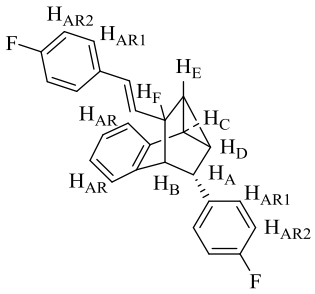

endo,trans-**10**

exo,endo,trans-**9**: colourless oil; R_f = 0.59 (petroleum ether /dichlormethane = 9:1); ^{1}H NMR ($CDCl_3$, 600 MHz) δ/ppm: 7.17-7.02 (m, 4H), 6.93-6.81 (m, 5H), 6.74-6.66 (m, 2H), 6.48 (m, 2H, H_H, H_A), 6.22 (d, 1H, *J* = 7.5 Hz, H_{AR}), 5.92 (dd, 1H, *J* = 15.5; 8.4 Hz, H_G), 5.30 (ddd, 1H, *J* = 9.4; 3.5; 1.7 Hz, H_B), 4.06 (t, 1H, *J* = 4.7 Hz, H_E), 3.41 (d, 1H, *J* = 8.4 Hz, H_F), 3.28-3.20 (m, 2H, H_C, H_D); ^{13}C NMR ($CDCl_3$, 150 MHz) δ/ppm: 150.0 (s), 139.6 (s), 139.1 (s), 135.2 (s), 134.8 (d), 132.5 (d), 132.1 (s), 131.7 (s), 129.4 (2d), 128.7 (d), 128.1 (2d), 127.3 (2d), 126.6 (2d), 126.4 (d), 126.3 (d), 126.1 (d), 125.8 (d), 125.2 (d), 120.9 (d), 58.4 (d), 53.9 (d), 46.2 (d), 45.8 (d); MS *m/z* (%, fragment) (EI): 370 (100, M^+); HRMS (*m/z*) for $C_{26}H_{20}F_2$: $[M+H]^+_{calcd}$ = 371.1533, $[M+H]^+_{found}$ = 371.1538.

endo,trans-**10**: colourless oil; R_f = 0.59 (petroleum ether/dichloromethane = 9:1); ^{1}H NMR ($CDCl_3$, 600 MHz) δ/ppm: 7.29-7.18 (m, 2H), 7.03-6.88 (m, 4H), 6.83-6.75 (m, 3H), 6.72-6.61 (m, 2H), 6.60 (d, 1H, *J* = 7.4 Hz, H_{AR}), 6.34 (d, 1H, *J* = 15.7 Hz, H_{et}), 5.30 (dd, 1H, *J* = 15.7; 7.4 Hz, H_{et}), 3.59-3.53 (m, 1H, H_A), 3.24-3.12 (m, 2H, H_F,H_B), 2.43 (t, 1H, *J* = 7.1 Hz, H_c), 2.01-1.93 (m, 1H,

$H_{D/E}$), 1.88-1.80 (m, 1H, $H_{D/E}$); MS *m/z* (%, fragment) (EI): 370 (100, M^+); HRMS (*m/z*) for $C_{26}H_{20}F_2$: $[M+H]^+_{calcd}$ = 371.1533, $[M+H]^+_{found}$ = 371.1522.

Declaration of interests

The authors declare that they have no known competing financial interests or personal relationships that could have appeared to influence the work reported in this paper.

Acknowledgements

The University of Zagreb short term scientific support (2019) under the title *Synthesis and functionalization of novel (hetero)polycyclic photoproducts as potential cholinesterase inhibitors* is The University of Zagreb short term scientific support (2019) under the title Synthesis and functionalization of novel (hetero)polycyclic photoproducts as potential cholinesterase inhibitors is gratefully acknowledged. The Higher Educational Institutional Excellence Program 2019 by the grant of the Hungarian Ministry for Innovation and Technology. (Grant Number: NKFIH-1158-6/2019) also supported this work. The computational resources were provided by the University of Zagreb Computing Centre (SRCE).

References

[1] I. Škorić, M Šmehil, Ž. Marinić, K. Molčanov, B. Kojić-Prodić, M. Šindler Kulyk, *J. Photochem. Photobiol. A - Chemistry*, **2009**, *207*, 190.

[2] R. C. Hahn, L .J. Rothman, *J. Am. Chem. Soc.* **1969**, *91*, 2409.

[3] Z. Goldschmidt, U. Gutman, *Tetrahedron*,**1974**, *30*, 3327.

[4] R. P. Johnson, A. Exarchou, Ch. W. Jeffrd, R.C. Hahn, *J. Org. Chem*., **1977**, *42*, 3758.

[5] D. Wege, *J. Org. Chem.*, **1990**, *55*, 1667.

[6] I. Kikaš, I. Škorić, Ž. Marinić, M. Šindler-Kulyk, *Tetrahedron*, **2010**, *66*, 9405.

[7] D. Vidaković, I. Škorić, M. Horvat, Ž. Marinić, M. Šindler-Kulyk, *Tetrahedron*, **2008**, *64*, 3928.

[8] N. Basarić, Ž. Marinić, M. Šindler-Kulyk, *J. Org. Chem*., **2006**, *71*, 9382.

[9] I. Škorić, N. Basarić, Ž. Marinić, A. Višnjevac, B. Kojić-Prodić, M. Šindler-Kulyk, *Chem. Eur. J.*, **2005**, *11*, 543.

[10] K. Butković, N. Basarić, K. Lovreković, Ž. Marinić, A. Višnjevac, B. Kojić-Prodić, M. Šindler-Kulyk, *Tetrahedron Lett.*, **2004**, *45*, 9057.

[11] I. Škorić, N. Basarić, Ž. Marinić, M. Šindler-Kulyk, *Heterocycles*, **2001**, *55*, 1889.

[12] M. Šindler-Kulyk, I. Škorić, S. Tomšić, Ž. Marinić, D. Mrvoš-Sermek, *Heterocycles*, **1999**, *51*, 1355.

[13] M. Šindler-Kulyk, G. Kragol, I. Piantanida, S. Tomšić, I. Vujković Cvijin, Ž. Marinić, B. Metelko, B., *Croat. Chem. Acta*, **1996**, *69*, 1593.

[14] I. Škorić, I. Kikaš, M. Kovács, L. Fodor, Ž. Marinić, K. Molčanov, B. Kojić-Prodić, O. Horváth, *J. Org. Chem*., **2011**, *76*, 8641.

[15] D. Vuk, D. Potroško, M. Šindler-Kulyk, Ž. Marinić, K. Molčanov, B. Kojić-Prodić, I. Škorić, *J. Mol. Struct.*, **2013**, *1051*, 1.

[16] D. Vuk, Ž. Marinić, I. Škorić, *Croat. Chem. Acta*, **2014**, *87*, 465.

[17] I. Šagud, M. Levačić, Ž. Marinić, I. Škorić, *Eur. J. Org. Chem*., **2017**, 3787.

[18] R. L. Rucker, B. J. Schwartz, M. A. El-Bayoumi, *Chem. Phys. Lett*., **1995**, *235*, 471.

[19] F. D. Lewis, X. Zuo, *Photochem. Photobiol. Sci*., **2003**, *2*, 1059.

[20] J. Saltiel, D. F. Jr. Sears, F. B. Mallory, C. W. Mallory, C. A. Buser, *J. Am. Chem. Soc*., **1986**, *108*, 1688.

[21] J. Saltiel, D. F. Jr. Sears, J.-O. Choi, Y.-P. Sun, D. W. Eaker, *J. Phys. Chem.* **1994**, *98*, 35.

[22] A. Ratković, Ž. Marinić, I. Škorić, *J. Mol. Struc*., **2018**, *1168*, 165.

[23] D. Vuk, K. Molčanov, I. Škorić, *J. Mol. Struc.*, **2014**, *1065*, 43.

[24] M. Šindler-Kulyk, Z. Stiplošek, D. Vojnović, B. Metelko, Ž. Marinić, *Heterocycles*, **1991**, *32*, 2357.

[25] R. Robiette, J. Richardson, V. K. Aggarwal, J. N. Harvey J. *Am. Chem. Soc.* **2006**, *128*, 2394.

[26] Y. Zhao, D. Truhlar *Theor. Chem. Acc.* **2008**, *120*, 215.

[27] Gaussian 09, Revision D.01, M. J. Frisch, G. W. Trucks, H. B. Schlegel, G. E. Scuseria, M. A. Robb, J. R. Cheeseman, G. Scalmani, V. Barone, G. A. Petersson, H. Nakatsuji, X. Li, M. Caricato, A. Marenich, J. Bloino, B. G. Janesko, R. Gomperts, B. Mennucci, H. P. Hratchian, J. V. Ortiz, A. F. Izmaylov, J. L. Sonnenberg, D. Williams-Young, F. Ding, F. Lipparini, F. Egidi, J. Goings, B. Peng, A. Petrone, T. Henderson, D. Ranasinghe, V. G. Zakrzewski, J. Gao, N. Rega, G. Zheng, W. Liang, M. Hada, M. Ehara, K. Toyota, R. Fukuda, J. Hasegawa, M. Ishida, T. Nakajima, Y. Honda, O. Kitao, H. Nakai, T. Vreven, K. Throssell, J. A. Montgomery, Jr., J. E. Peralta, F. Ogliaro, M. Bearpark, J. J. Heyd, E. Brothers, K. N. Kudin, V. N. Staroverov, T. Keith, R. Kobayashi, J. Normand, K. Raghavachari, A. Rendell, J. C. Burant, S. S. Iyengar, J. Tomasi, M. Cossi, J. M. Millam, M. Klene, C. Adamo, R. Cammi, J. W. Ochterski, R. L. Martin, K. Morokuma, O. Farkas, J. B. Foresman, and D. J. Fox, Gaussian, Inc., Wallingford CT, 2009.

[28] C. A. Hunter, K. M. Sanders, *J. Am. Chem. Soc.*, **1990**, *112*, 5525.

[29] J. Nishimura, Y. Nakamura, Y. Hayashida, T. Kudo, *Acc. Chem. Res.*, **2000**, *33*, 679.

[30] E. A. Meyer, R. K. Castellano, F. Diederich, *Angew. Chem.*, **2003**, *15*, 1244; *Angew. Chem. Int. Ed.*, **2003**, *42*, 1210.

[31] I. Škorić, I. Kikaš, M. Kovács, M. Šindler-Kulyk, O. Horváth, *J. Photochem. Photobiol. A - Chemistry*, **2010**, *211*, 152.

[32] F. Bangerter, M. Karpf, L. A. Meier, P. Rys, P. Skabal, *J. Am. Chem. Soc.* **1998**, *120*, 10653.